Journal of Medicinal Chemistry Article

J. Med. Chem. **2010,** *53,* 4779–4792 **4779**
DOI: 10.1021/jm100438s

Structure-Based Drug Design and Optimization of Mannoside Bacterial FimH Antagonists

Zhenfu Han,[†,∥] Jerome S. Pinkner,[‡,∥] Bradley Ford,[§,∥] Robert Obermann,[†] William Nolan,[†] Scott A. Wildman,[†] Doug Hobbs,[†] Tom Ellenberger,[†] Corinne K. Cusumano,[‡] Scott J. Hultgren,*[,‡] and James W. Janetka*[,†]

[†]*Department of Biochemistry and Molecular Biophysics,* [‡]*Department of Molecular Microbiology, Center for Women's Infectious Disease Research, and* [§]*Department of Pathology and Immunology, Washington University School of Medicine, 660 S. Euclid Avenue, St. Louis, Missouri 63110.* [∥] *These authors contributed equally to the work.*

Received April 9, 2010

FimH-mediated cellular adhesion to mannosylated proteins is critical in the ability of uropathogenic *E. coli* (UPEC) to colonize and invade the bladder epithelium during urinary tract infection. We describe the discovery and optimization of potent small-molecule FimH bacterial adhesion antagonists based on α-D-mannose 1-position anomeric glycosides using X-ray structure-guided drug design. Optimized biarylmannosides display low nanomolar binding affinity for FimH in a fluorescence polarization assay and submicromolar cellular activity in a hemagglutination (HA) functional cell assay of bacterial adhesion. X-ray crystallography demonstrates that the biphenyl moiety makes several key interactions with the outer surface of FimH including $\pi-\pi$ interactions with Tyr-48 and an H-bonding electrostatic interaction with the Arg-98/Glu-50 salt bridge. Dimeric analogues linked through the biaryl ring show an impressive 8-fold increase in potency relative to monomeric matched pairs and represent the most potent FimH antagonists identified to date. The FimH antagonists described herein hold great potential for development as novel therapeutics for the effective treatment of urinary tract infections.

Introduction

FimH is the adhesive component of the type 1 pilus, which is a member of the chaperone/usher pathway (CUP[a]) family of pilus gene clusters. CUP pili function in colonization, in biofilm formation, and for gaining entry into host cells.[1] FimH is assembled into the tips of type 1 pili, which are essential virulence factors for the establishment of *Escherichia coli* urinary tract infections (UTIs). FimH mediates the colonization and invasion of the bladder epithelium.[2] After invasion, UPEC are expelled back out of the bladder cell in a Tlr4 dependent process[2c] or they escape into the cytoplasm where they rapidly replicate into intracellular bacterial communities (IBCs).[3] IBC formation is transient and allows the rapid expansion of a single invaded bacterium into tens of thousands of bacteria aggregated into a biofilm-like mass in a single bladder cell. Upon dispersal of UPEC from the IBC biomass, they are capable of spreading to neighboring cells to repeat the process, thus further increasing the bacterial load in the bladder.[4] Blocking FimH binding to mannosylated proteins with FimH antibodies or small molecules is sufficient to prevent bacterial entry and infection, thus providing the therapeutic rationale for developing novel FimH-binding drugs for the treatment of UTIs.[5] We and others have recently reported the discovery that α-D-mannosides and glycoconjugate dendrimers thereof bind with high affinity to the bacterial lectin FimH[6] and prevent hemagglutination of red blood cells mediated by cross-linking of surface epitopes containing mannose. Ligand binding affinities have been obtained using diverse quantitative binding assays and confirmed with the X-ray crystal structure of various mannosides, such as α-D-butylmannoside (Butylαman), bound to FimH.[6a]

Long chain alkyl- and arylmannosides display the highest affinity of the monovalent ligands likely due to increased hydrophobic interactions with Ile-52 and two tyrosine residues, Tyr-48 and Tyr-137, lining the hydrophobic rim of the binding pocket. A separate crystal structure of the FimH receptor binding domain bound to oligomannose-3 was recently solved[6c] that reveals an "open gate" between Tyr-48 and Tyr-137 into which oligomannose-3 inserts, adopting a conformation in which the second mannose residue interacts with Tyr-48. Interestingly, the latter conformation is different from that seen in monomannose-bound forms of FimH. This conformational flexibility of the tyrosine residues seen in these X-ray structures provides a rationale for designing arylmannosides with increased binding affinity relative to alkylmannosides by introducing additional hydrophobic and ring stacking interactions with Tyr-48 or Tyr-137.

With the exception of one recent communication,[6k] all efforts described have only been focused on glycoconjugate dendrimers. Although synergistic avidity or a "cluster effect"[6b] can be realized with the latter agents, multivalent ligands are predicted to be poorly permeable to the GI tract and likely not amenable for oral dosing because of their large

*To whom correspondence should be addressed. For J.W.J.: phone, 314-362-0509; fax, 314-362-7183; e-mail, janetkaj@wustl.edu. For S.J.H.: phone, 314-362-7059; fax, 314-362-1998; e-mail, hultgren@biocrim.wustl.edu.

[a]Abbreviations: UTI, urinary tract infection; UPEC, uropathogenic *E. coli*; SAR, structure−activity relationship; HA, hemagglutination; HAI, HA inhibition; FAM, fluoroscein amidite; SPR, surface plasmon resonance; CUP, chaperone/usher pathway; IBCs, intracellular bacterial communities; Butylαman, α-D-butylmannoside; Methylαman, α-D-methylmannoside; MeUmbαman, 4-methylumbellferyl-α-D-mannoside; Heptylαman, α-D-heptylmannoside; Phenylαman, α-D-phenylmannoside; PD, pharmacodynamic; PK, pharmacokinetic.

Published on Web 05/27/2010

Scheme 1[a]

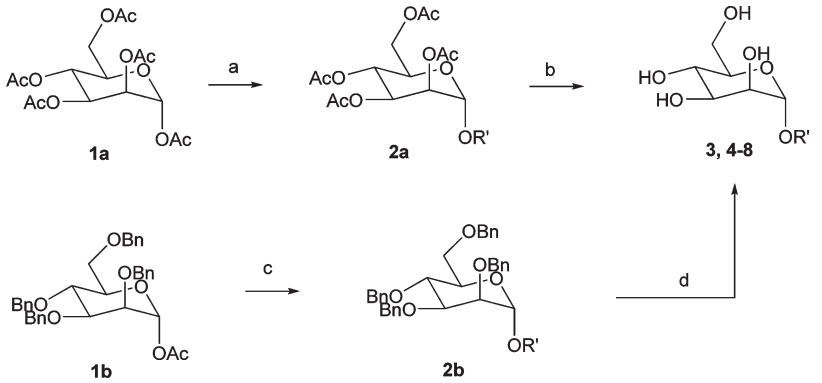

[a] Reagents and conditions: (a) R′OH, BF_3OEt_2, CH_2Cl_2, reflux; (b) (i) NaOMe, MeOH; (ii) H^+ exchange resin; (c) R′OH, BF_3OEt_2, CH_2Cl_2, 0 to 25 °C; (d) H_2, 10% Pd/C, EtOH, EtOAc.

Table 1. SAR of Simple Aryl Substitution Mannoside Library

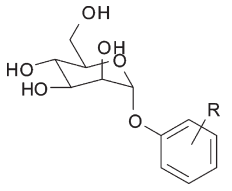

compd	R	HAI titer (μM)	compd	R	HAI titer (μM)
3a	H	30	**3m**	2-CN	6
3b	4-NO_2	31	**3n**	3-CN	23
3c	3-NO_2	16	**3o**	4-CN	30
3d	4-NH_2	32	**3p**	4-OMe	8
3e	3-Me	4	**3q**	2-NHAc	125
3f	4-Me	8	**3r**	3-NHAc	12
3g	2-Cl	4	**3s**	4-NHAc	8
3h	3-Cl	8	**3t**	3-$CONH_2$	16
3i	4-Cl	32	**3u**	4-$CONH_2$	15
3j	3-CO_2Me	6	**3v**	3-OAc	16
3k	4-CO_2Me	8	**3w**	4-CH_2CO_2Me	30
3l	3-CO_2H	60	**4**	3, 5-CO_2Me	2

molecular weight and high polarity. Therefore, we were interested in rationally improving both binding affinity and cellular potency by optimization of monovalent FimH mannoside antagonists for the clinical treatment of urinary tract infections.

Results and Discussion

Arylmannoside inhibitors of hemagglutination were first reported over 2 decades ago,[7] but surprisingly only limited structure−activity relationships (SAR) of monovalent arylmannosides are known,[6k,7] so we designed and synthesized a diverse compound set based on aryl substitution of α-D-phenylmannoside (Phenylαman). As shown in Scheme 1, α-D-mannoside derivatives were prepared using traditional Lewis acid mediated glycosidation.[8] Reaction of acylated α-D-(+)-mannose **1a** with a variety of phenols and BF_3OEt_2 resulted in exclusive formation of the α-isomer mannosides **2**. Subsequent deacylation with NaOMe in methanol gave the desired arylmannosides **3**−**8** in good yield. Biological activity against FimH was evaluated using a guinea pig red blood cell-based HA assay[9] in which HA inhibition (HAI) titers are defined as the concentration of the compound that results in >90% HA inhibition.

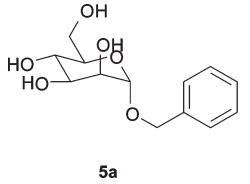

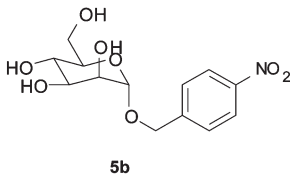

Figure 1. Benzylmannosides.

This assay was preferred to a simple FimH binding assay for screening and developing SAR, since it assesses the compound's ability to prevent bacterially mediated adhesion directly in a cellular assay. As shown in Table 1, we found the general trend that 2- and 3-substitution was optimal for potency relative to 4-substitution in most examples with the exception of the acylanilines **3q**−**s** in which this trend was dramatically reversed. Ortho-substituted chlorophenyl **3g**, cyanophenyl **3m**, and meta-substituted methyl ester **3j** all showed an impressive greater than 5-fold improvement in potency relative to parent phenylmannoside **3a**. Interestingly, carboxylic acid **3l** lost 10-fold potency relative to matched pair methyl ester **3j** showing an HAI titer of only 60 μM. Incorporation of an additional methyl ester in the 5-position of **3j**, as with compound **4**, resulted in a relatively large 3-fold enhancement in potency. Benzylic analogues **5a** and **5b** (Figure 1), which have different conformational space and flexibility relative to direct phenyl substitution of the anomeric oxygen, as with matched pairs **3a** and **3b**, show a 2-fold decrease (HAI titer of 60 μM) in potency.

Upon examination of the X-ray structures of Butylαman and oligomannose-3 coupled with docking studies with mannoside diester **4** bound to FimH, we were encouraged that further improvements in binding affinity could be achieved by addition of a second aryl or aliphatic ring system in anticipation of introducing either additional hydrophobic or $\pi-\pi$ stacking interactions with Tyr-48 and/or Tyr-137 as seen from the directionality of the butyl side chain seen in the Butylαman structure and position of the second mannose residue in the oligomannose-3 bound conformation.

To this end, we explored analogues with an additional ring system directly attached or fused ring to the parent arylmannosides of Table 1. We discovered that a variety of ring systems were tolerated (Table 2) relative to the previously described coumarin analogue 4-methylumbellferyl-α-D-mannoside **6** (MeUmbαman).[7] The most attractive inhibitor in this series of compounds was the 4′-biphenyl derivative **8e**

Table 2. SAR of Multiring System Analogues

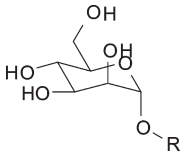

compd	R	HAI titer (μM)	compd	R	HAI titer (μM)
6	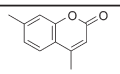	2	**8b**	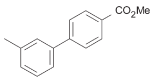	6
7a	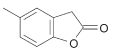	8	**8c**	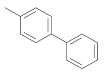	8
7b		6	**8d**	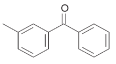	8
7c	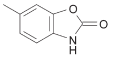	4	**8e**	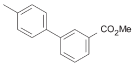	1
7d	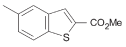	2	**8f**	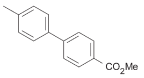	4
7e	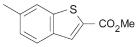	2	**8g**		2
8a		62	**8h**	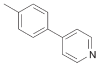	2

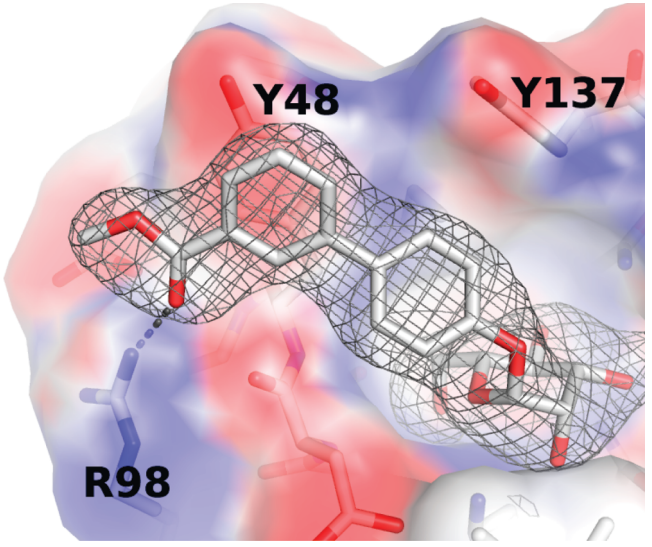

Figure 2. X-ray structure of mannoside **8e** (PDB code 3MCY) with electron density (mesh) calculated with $2F_o - F_c$ coefficients, contoured at 1σ. Interaction with the Arg-98−Glu-50 salt bridge (dashes), $\pi-\pi$ stacking with Tyr-48, and hydrophobic interaction with Tyr-137 are shown. Surface electrostatic potential of FimH, calculated with APBS,[10] is displayed such that pure blue and red would be $+4kT/e$ and $-4kT/e$, respectively.

bearing a methyl ester off the meta position of the second aryl ring and showing a 2-fold improvement relative to **6** having an HAI titer of 1 μM. In order to determine the source of this potency enhancement and aid in further improvements, we obtained a high-resolution X-ray crystal structure of **8e** bound to FimH. Shown in Figure 2, inhibitor **8e** binds in a very complementary "lock and key" fashion to the FimH binding pocket. The mannose ring is making conserved interactions with the mannose-binding pocket similar to those previously

Scheme 2[a]

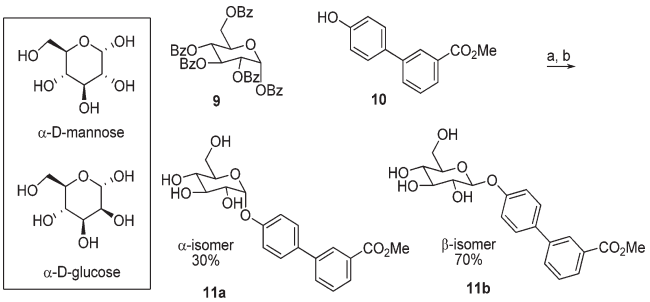

[a] Reagents and conditions: (a) R′OH, BF_3OEt_2, CH_2Cl_2, reflux; (d) NaOMe, MeOH.

reported in the structure of α-D-mannose,[2g] while the two aromatic rings of the biphenyl moiety exist in a nonplanar conformation allowing for π-stacking and hydrophobic interactions with Tyr-48 and other residues encompassing the exterior hydrophobic cleft of FimH. The π-stacking interaction with Tyr 48 occurs on the opposite side of the phenyl ring from that engaged by oligomannose-3, which inserts itself into the open "tyrosine gate" formed by Tyr-48 and Tyr-137. Thus, **8e** engages the "tyrosine gate" in a way that results in alteration of the extended FimH binding pocket through closure of the tyrosine gate upon rotation of Tyr-48. This binding mode places the ester of **8e** within H-bonding distance to a salt bridge formed between Arg-98 and Glu-50 (Figure 2). It is noteworthy that the HAI titer for Methylαman is >1 mM, making compound **8e** greater than 1000-fold more potent from the addition of the biphenyl ester.

The latter observation led us to investigate replacing the mannose with alternative sugars or mimics, since the biphenyl portion alone provides a significant contribution to biological activity presumably from tighter binding to FimH. We decided to start by replacing the mannose portion of **8e** with glucose, since all chiral centers are identical except for the 3-hydroxyl group adjacent to the anomeric center, being of *R* stereochemistry in mannose and *S* in glucose (Scheme 2). Standard Lewis acid mediated glycosidation gave isomeric mixtures at the anomeric center favoring the undesired β-isomer, conversely to the clean formation of the α-isomer seen for the mannosides. Correspondingly, reaction of benzoyl protected α-D-glucose **9** with phenol **10** using BF_3OEt_2 followed debenzoylation yielded both the α-D-glucoside **11a** and β-D-glucoside **11b** in a 3:7 ratio. Unfortunately, neither glucoside isomer showed any activity in the hemagglutination assay even up to 2.5 mM. Therefore, modification of a single chiral hydroxyl group stereocenter on the mannoside is sufficient to significantly decrease biological activity, presumably resulting from the inability to tightly bind FimH. Upon analysis of the specific interactions realized from α-D-mannose bound to FimH,[2g] this hydroxyl group is involved in a H-bonding interaction with the N-terminal residue of FimH and a water molecule contained inside the binding pocket. In any event, this finding demonstrates the exquisite specificity of FimH for mannose epitopes, which has enabled UPEC bacteria to exclusively recognize mannose-presenting cells.

Next, we returned our attention to optimizing the biaryl portion of the mannoside by undertaking an extensive SAR evaluation of the second ring through a modified Topliss-type[11] evaluation of substituents. We designed this focused set

Scheme 3[a]

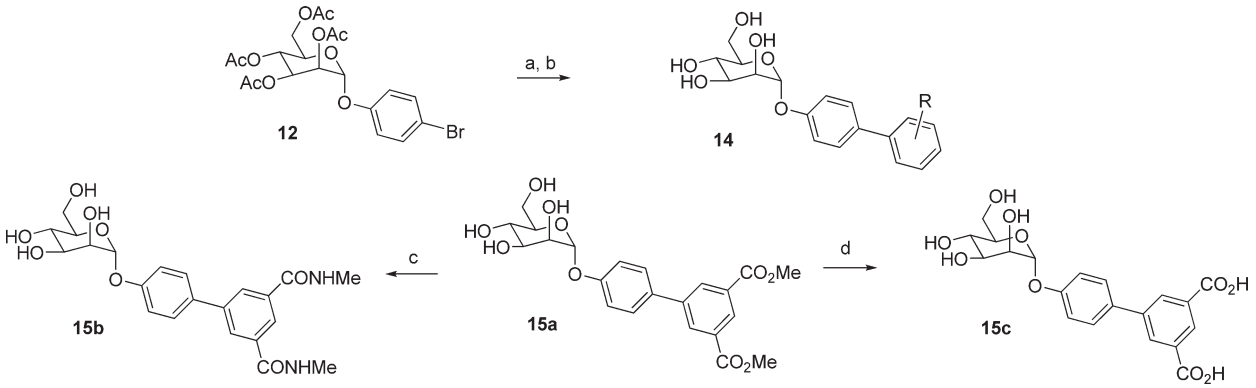

[a] Reagents and conditions: (a) RPh-B(OR)$_2$, Pd(Ph$_3$P)$_4$, dioxane/water (4:1), Cs_2CO_3, 80 °C; (b) NaOMe, MeOH; (c) H_2NMe, EtOH; (d) NaOH (aq), MeOH.

Table 3. SAR of Substituted Biphenylmannosides

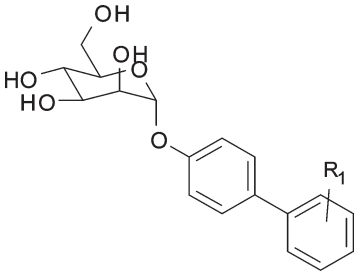

compd	R_1	HAI titer (μM)	compd	R_1	HAI titer (μM)
14a	3-CONHMe	1	**14o**	2-$NHSO_2Me$	12
14b	3-NHAc	2	**14p**	3-$NHSO_2Me$	2
14c	3-CO_2H	4	**14q**	2-SO_2NHMe	4
14d	2-CN	2	**14r**	3-SO_2NHMe	1
14e	3-CN	1	**14s**	3-NO_2	0.5
14f	4-CN	8	**14t**	4-NO_2	2
14g	2-CH_2OH	16	**14u**	2-$CONH_2$	6
14h	3-CH_2OH	3	**14v**	3-$CONH_2$	2
14i	4-CH_2OH	6	**14w**	2-CF_3	8
14j	2-OH	8	**14x**	3-CF_3	2
14k	3-OH	4	**14y**	3-F	6
14l	4-OH	6	**15a**	3, 5-CO_2Me	0.15
14m	2-OMe	1	**15b**	3, 5-CONHMe	0.37
14n	3-OMe	1.5	**15c**	3, 5- CO_2H	2

of compounds with some bias toward improving interactions with Arg-98 and Glu-50 but also were interested in elucidating the importance of ring electronic properties as a means to improve the stacking interaction with Tyr-48. A few initial analogues were prepared using the synthetic route outlined previously in Scheme 1, but we developed a more convergent synthesis based on Suzuki coupling of aryl bromide intermediate **12** as shown in Scheme 3. By employment of standard Suzuki conditions by reaction of arylboronic acids or esters with Pd(Ph$_3$P)$_4$ and Cs_2CO_3, **12** was converted to protected biphenylmannosides **13** in good yield. The acylated biarylmannosides **13** were then deprotected as before to generate the final target compound **14** or **15a** displayed in Table 3. Diester **15a** was further functionalized to dimethylamide **15b** by reaction with dimethylamine or converted to diacid **15c** by basic hydrolysis in methanol. Upon evaluation of HA titers, the matched pair meta-substituted methylamide **14a** was equipotent to ester **8e** while reverse amide **14b** and free acid **14c** displayed moderately lower potencies of 2 and 4 μM, respectively. The latter result was surprising, since these modifications were designed to introduce an electrostatic interaction with Arg-98 and to disrupt the Arg-98/Glu-50 salt bridge. On the other hand, sulfonamide **14r** has equivalent potency to carboxamide **14a**, providing further evidence that a hydrogen bond acceptor is required for optimal potency presumably from interaction with Arg-98. Upon analysis of ortho, meta, and para matched pairs, it was obvious that para substitution was least preferred for activity while meta substitution was preferred to ortho substitution. This preference for meta substitution was most pronounced with the methyl alcohols **14g** and **14h** where the ortho analogue **14g** was over 5-fold less potent with an HAI titer of only 16 μM. We surmise that this large substituent results in an increased rotation of the two rings out of the plane, causing a nonproductive alignment for interactions with Tyr-48. Although a majority of the analogues tested contained electron withdrawing groups, in general electron donating groups such as the methyl alcohols **14g**−**i** and phenols **14j**−**l** were less active in the HA titer assay. The most

Scheme 4[a]

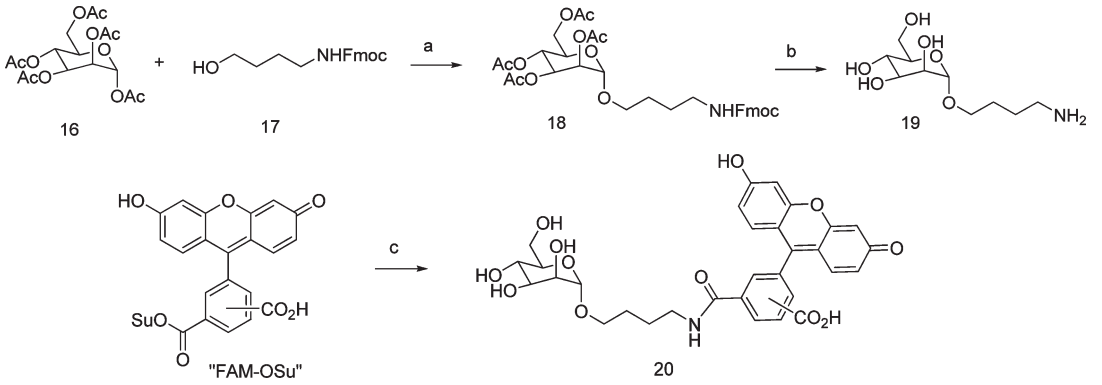

[a] Reagents and conditions: (a) BF_3OEt_2, CH_2Cl_2, reflux; (b) (i) NaOMe, MeOH; (c) **19**, Et_3N, DMF.

Table 4. Binding Affinity of Selected Mannosides in Fluorescence Polarization Assay

compd	FP binding EC_{50} (μM)	HAI titer (μM)	compd	FP binding EC_{50} (μM)	HAI titer (μM)
6 (MeUmbαman)	0.044	2	Heptylαman	0.089	15
8e	0.052	1	**4**	0.091	2
8f	0.059	4	**14p**	0.097	2
3k	0.064	8	**14c**	0.099	4
14b	0.07	2	**3a**	0.114	30
14a	0.075	1	**3s**	0.122	8
15a	0.077	0.15	**3r**	0.160	12
14v	0.078	2	**3n**	0.162	23
3j	0.084	6	**5a**	0.187	60
15b	0.087	0.37	Butylαman	0.245	125

potent of the monosubstituted mannosides is meta nitro derivative **14m** with an HAI titer of 0.5 μM. One possible explanation for the improved potency of **14m** is that the partial negative charge on the nitro oxygen atoms allow for an optimized H-bond acceptor−donor interaction with Arg-98 coupled with the increased electron withdrawing ability of the nitro group possibly enhancing stacking interactions with Tyr-48.

Perhaps the most exciting finding from this study was that addition of another ester or amide substituted in the other meta position such as diester **15a** and dimethylamide **15b** resulted in the two most potent mannoside inhibitors of FimH with activities of 150 and 370 nM, respectively. With respect to diester **15a** this constitutes a 7-fold improvement in activity relative to mono ester **8e**. The diamide **15b**, while slightly less potent, has much improved solubility relative to diester **15a**. We hypothesize that the addition of the second ester or amide serves a 2-fold purpose for improving activity. First, we propose that the electron withdrawing group results in less electron density of the aryl ring, thus improving $\pi-\pi$ stacking interactions with Tyr-48. Second, the monoester (or amide) analogue can presumably access conformations in which the aryl ring is not in proximity to Arg-98 whereas the meta diester (or diamide) analogue likely exists only in conformations where the ester or amide resides in proximity to Arg-98 resulting in less entropic loss upon binding and a lower energy bound conformation resulting in increased binding affinity and potency.

In order to more accurately determine the relative contributions of binding affinity to FimH versus other compound properties to the potency seen in the cellular HA assay, we developed a high-throughput fluorescence polarization/anisotropy competitive binding assay using a fluorescent-labeled mannoside ligand shown in Scheme 4. Synthesis was achieved as before using Lewis acid mediated glycosylation with protected amino alcohol **17** followed by dual Fmoc and acyl deprotection of intermediate **18** to give free amine **19**. Subsequent reaction of 5(6)FAM-OSu with **19** using triethylamine in DMF gave the desired fluorescently tagged FAM-mannoside **20**.

The K_D for FAM mannoside **20** was measured to be 0.17 μM, while the HAI titer was much lower at 125 μM. We evaluated 20 mannoside ligands with structural diversity and activities in the HA cell assay ranging from 150 nM to 125 μM for their ability to competitively inhibit binding of 5(6)-FAM **20**. Interestingly, we found that all potently competed for FimH binding having EC_{50} less than 0.25 μM but having no clear correlation of EC_{50} with the activity found in the HA cell assay (Table 4). Although there was over a 60-fold range in cellular potency, there was only about a 5-fold range in binding affinity (Table 5). In addition, there was also no linear correlation of data with the two assays. Simple alkylmannosides have the highest drop in cell activity, as demonstrated with Butylαman having the most dramatic difference with a 510-fold drop in cell activity relative to binding.

Interestingly, the optimized biphenylmannoside series shows a modest correlation of binding affinity having a much smaller drop in cell activity relative to binding. The diester **15a** and diamide **15b** show the best correlation with only a 2-fold and 4-fold difference in cell potency vs binding. It is important to note that even though these two analogues are the most potent in the HA assay, they have about 2-fold less binding affinity in the FP assay than the tightest binding mannosides. While it is unclear why there is no correlation of binding to activity in the cell, there is a moderate correlation when compounds with binned affinities are compared. However, the latter observation cannot explain the nonlinear increase in cell activity of **15a** and **15b** relative to the monosubstituted biphenylmannosides. Perhaps differential binding kinetics including varied ON rates and OFF rates of mannoside analogues to FimH can provide a plausible explanation for the

Table 5. Correlation of HAI Titer and FimH Binding Data

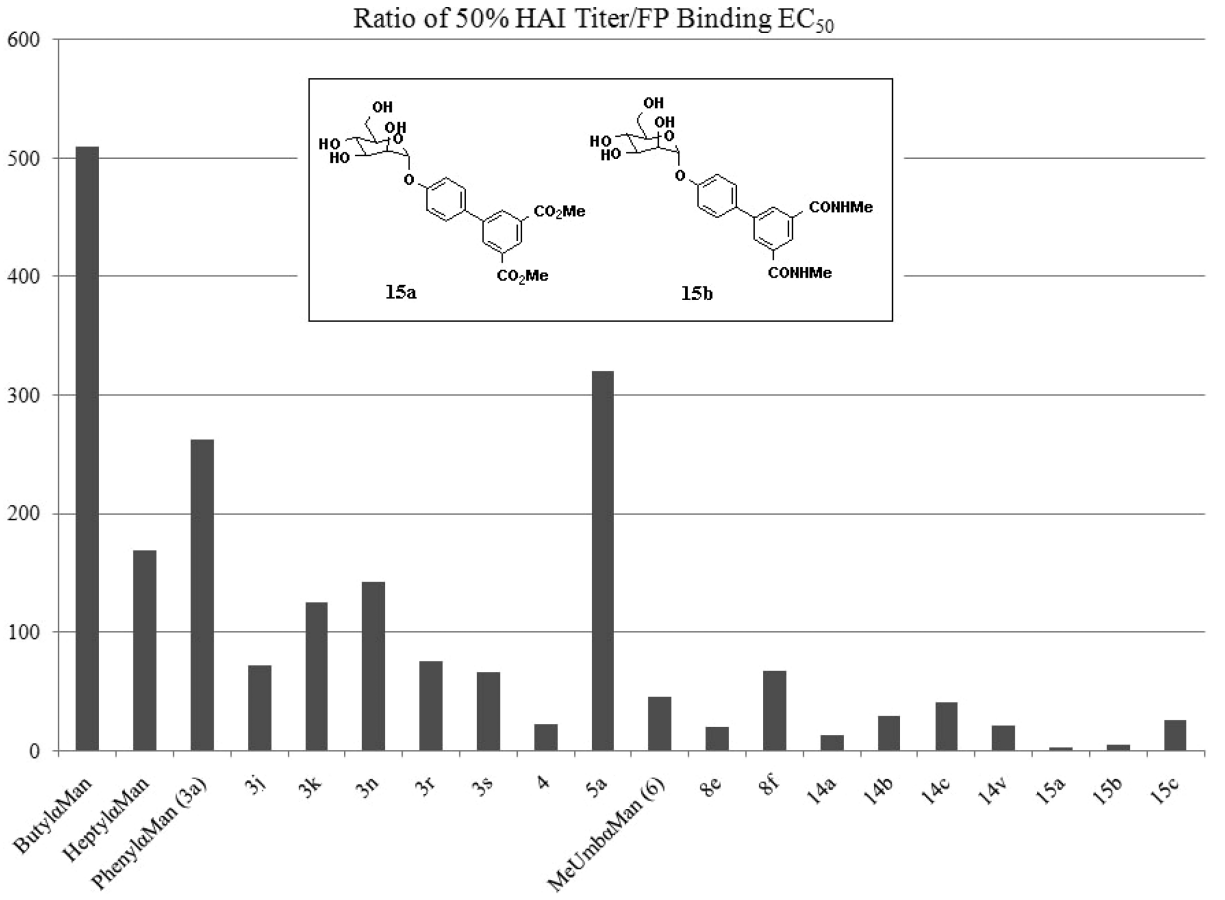

latter. It is worth mentioning that the previously reported K_D values[6a] obtained through surface plasmon resonance (SPR) for **6** (MeUmbαman), Butylαman, and Heptylαman are 20, 151, and 5 nM, respectively. While the result for Butylαman is similar, the FP assay suggests that MeUmbαman is the most potent (44 nM), being 2-fold more potent than Heptylαman (89 nM). Considering the lack of correlation between binding affinity and biological activity in the cell plus the variability seen comparing two separate binding assays, the HA assay coupled with the use of structural information is a preferred route for medicinal chemistry optimization of mannoside FimH ligands. Nonetheless, based on the HAI titer cellular data, mannoside **15a** is the most potent FimH antagonist reported to date and represents an excellent lead candidate for further optimization of the monovalent mannosides toward a novel preclinical candidate with tremendous therapeutic potential for treating urinary tract infections. Several compounds show pharmacodynamic (PD) activity in novel murine models of UTI and are currently being optimized for in vivo efficacy and pharmacokinetic (PK) properties. The results of these studies will be reported shortly in a future manuscript.

The development of multivalent and dendrimeric mannosides has been the major focus of previous work on FimH antagonists because simple mannosides, while having respectable binding affinity to FimH, show poor cellular activity in the HA assay. It has been demonstrated that multivalent mannosides are effective at increasing avidity through a phenomenon termed "cluster effect" resulting in an overall increased binding affinity when calculated per mannoside monomer. Therefore, we were curious if our improved monovalent mannosides **15a** and **15b** would produce a similar increase in avidity or cluster effect previously reported for dendrimeric mannosides. For synthetic simplicity, we chose to utilize a model system based on monoamide **14a**. A symmetrical divalent mannoside was designed by connecting two monomers via an amide based linker to the two biphenyl rings (Scheme 5). Accordingly, dimeric inhibitors based on **14a** were synthesized by coupling carboxylic acid **13c** to either diamine 2-(2-aminoethoxy)ethanamine or 2-[2-(2-aminoethoxy)ethoxy]ethanamine, yielding diamide **21** or diamide **22**, respectively, using standard HATU coupling conditions with Hunig's base in DMF. The shorter chain analogue **21** showed an HAI titer of 0.75 μM, thus showing no noticeable improvement relative to **14a**, while the longer ethylene glycol linked diamide **22** displayed an almost 8-fold increase in activity with an impressive HAI titer of 130 nM. This constitutes a 4-fold increase in avidity relative to the expected potency of 500 nM based on two monomeric units of **14a**. In addition to increased potency, **22** has much improved solubility relative to **21**, making it an ideal starting point for further optimization. Although they are less likely to be effective as oral agents compared with the monovalent mannosides, the divalent mannosides are very useful chemical research tools and can potentially be developed into topical or intravenously dosed antibacterial agents. We are currently exploring optimized divalent analogues based on disubstituted **15b** which are predicted to have low nanomolar activity in the HA titer assay based on our current knowledge and understanding of SAR.

Scheme 5[a]

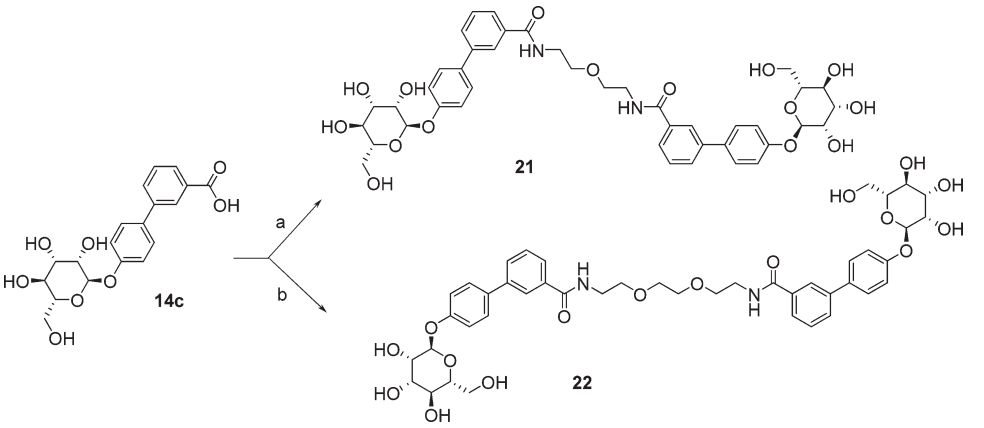

[a] Reagents and conditions: (a) HATU, $[H_2N(CH_2)_2]_2O$, DIPEA, DMF; (b) HATU, $[H_2N(CH_2)_2OCH_2]_2$, DIPEA, DMF.

Conclusions

We have designed a series of potent small-molecule FimH antagonists using the weak inhibitor α-D-phenylmannoside as an initial starting point for X-ray structure-guided optimization. Addition of substituents with increased hydrophobicity resulted in potency enhancements most pronounced using aromatic groups. Upon several rounds of SAR evaluation and optimization, we discovered that 4′-biaryl groups substituted on the meta position with H-bond acceptors such as esters or amides yield the most potent analogues. The structural basis for the enhanced potency results from both an optimal π-stacking arrangement of the biaryl moiety with Tyr-48 and an H-bonding interaction between an H-bond acceptor such as an amide carbonyl with Arg-98. We have also designed dimers derived from these mannosides, which show a 4-fold increase in cellular potency relative to that expected from 2 monomeric units. This improvement in avidity can be attributed to the ability of the dimer to bind two separate FimH molecules either from adjacent bacterial pili or on another bacterium. This is similar to the "cluster effect" of dendrimeric mannosides described recently by others. Both the optimized monomeric and dimeric mannosides described herein represent the most potent FimH antagonists reported to date and are very attractive leads as novel therapeutics for the treatment of urinary tract infections in which there exists a large unmet medical need. FimH mediated recognition of uroplakin receptors through the mannose binding epitope and subsequent invasion of UPEC into bladder cells is only one of a vast number of adhesion mechanisms involving a diverse range of carbohydrate epitopes which both bacterial and viral pathogens utilize for colonization.[12] The ability to design and optimize carbohydrate-derived or glycomimetic antagonists utilizing X-ray structure-based design strategies, such as described for FimH in this report, is instrumental for identifying other antagonists of carbohydrate−protein interactions and antivirulence therapeutics. It is important to mention that several carbohydrate-derived or glycomimetic drugs either are being evaluated in clinical trials or have reached the marketplace for the treatment of various diseases.[13] In fact, 1,6-bis[3-(3-carboxymethylphenyl)-4-(2-α-D-mannopyranosyloxy)phenyl]-hexane (TBC1269), a dimeric biarylmannoside antagonist[14] of E, P-, and L-selectin, is currently undergoing phase IIa evaluation for the treatment of asthma and psoriasis. We are currently pursuing the further optimization and preclinical evaluation of the biarylmannoside class of FimH antagonists primarily focused on improvements in pharmacokinetics and in vivo efficacy in animal models, which will be reported in another communication.

Experimental Section

General. ^{1}H NMR spectra were obtained on a Varian 300 MHz NMR instrument. The chemical shifts were reported as δ ppm relative to TMS, using residual solvent peak as the reference unless otherwise noted. The following abbreviations were used to express the multiplicities: s = singlet; d = doublet; t = triplet; q = quartet; m = multiplet; br = broad. High-performance liquid chromatography (HPLC) was carried out on a GILSON GX-281 using Waters C18 5 μM, 4.6 mm × 50 mm and Waters Prep C18 5 μM, 19 mm × 150 mm reverse phase columns. Mass spectra (MS) were obtained on a Waters MicromassZQ. All reactions were monitored by thin layer chromatography (TLC) carried out on Merck silica gel plates (0.25 mm thick, 60F254), visualized by using UV (254 nm) or dyes such as $KMnO_4$, *p*-anisaldehyde, and CAM (ceric ammonium molybdate). Silica gel chromatography was carried out on an ISCO system using ISCO prepacked silica gel columns (12−330 g sizes). All compounds used for biological assays are at least of 95% purity based on HPLC analytical results monitored with 220 and 254 nm wavelengths, unless otherwise noted. All reagents and solvents were purchased from commercially available sources and used as received except resorcinol monoacetate, which was purified prior to use. Phenyl-α-D-mannopyranoside, *p*-nitrophenyl-α-D-mannopyranoside, *p*-aminophenyl-α-D-mannopyranoside, and 4-methylumbelliferyl-α-D-mannopyranoside were purchased from Sigma.

Synthesis of Mannosides. General Procedure for the Preparation of Mannosides Using α-D-Mannose Pentaacetate: Methyl 3-[4-[(2*R*,3*S*,4*S*,5*S*,6*R*)-3,4,5-Trihydroxy-6-(hydroxymethyl)tetrahydropyran-2-yl]oxyphenyl]benzoate (8e). Methyl 3-[4-[(2*R*,3*S*,4*S*,5*R*,6*R*)-3,4,5-Triacetoxy-6-(acetoxymethyl)tetrahydropyran-2-yl]oxyphenyl]benzoate. Under nitrogen atmosphere, at 0 °C boron trifluoride diethyl etherate (0.128 g, 0.90 mmol) was added dropwise into a solution of α-D-mannose pentaacetate (0.120 g, 0.3 mmol) and methyl 3-(4-hydroxyphenyl)benzoate (0.140 g, 0.6 mmol) in 6 mL of CH_2Cl_2. After a few minutes the mixture was heated to reflux and was kept stirring for more than 36 h. The reaction was then quenched with water and extracted with CH_2Cl_2. The CH_2Cl_2 layer was collected, dried with Na_2SO_4, and concentrated in vacuo. The resulting residue was purified by silica gel chromatography with hexane/ethyl acetate combinations as eluent, giving rise to methyl 3-[4-[(2*R*,3*S*,4*S*,5*R*,6*R*)-3,4,5-triacetoxy-6-(acetoxymethyl)tetrahydropyran-2-yl]oxyphenyl]benzoate (0.136 g) in 81% yield. ^{1}H NMR (300 MHz, $CDCl_3$) δ ppm 8.23 (m, 1H), 7.99 (m, 1H), 7.74 (m, 1H), 7.57 (m, 2H), 7.50 (t, J = 7.8 Hz, 1H), 7.18 (m, 2H), 5.59 (dd, J = 3.6, 9.9 Hz, 1H), 5.58 (d, J = 1.5 Hz,

1H), 5.48 (dd, J = 2.1, 3.3 Hz, 1H), 5.39 (t, J = 10.2 Hz, 1H), 4.30 (dd, J = 5.4, 12.3 Hz, 1H), 4.06−4.15 (m, 2 H), 3.95 (s, 3H), 2.15 (s, 3H), 2.06 (s, 3H), 2.05 (s, 3H), 2.04 (s, 3H). MS (ESI): found $[M + H]^+$, 559.1.

Methyl 3-[4-[(2*R*,3*S*,4*S*,5*S*,6*R*)-3,4,5-Trihydroxy-6-(hydroxymethyl)tetrahydropyran-2-yl]oxyphenyl]benzoate (8e). Methyl 3-[4-[3,4,5-triacetoxy-6-(acetoxymethyl)tetrahydropyran-2-yl]oxyphenyl]benzoate (0.120 g) was stirred in 6 mL of methanol with a catalytic amount of sodium methoxide (0.02 M) at room temperature overnight. H^+ exchange resin (DOWEX 50WX4-100) was added to neutralize the mixture. The resin was filtered off and the filtrate was concentrated and then dried in vacuo, giving rise to pure product **8e** (0.084 g) in quantitative yield. ^{1}H NMR (300 MHz, CD_3OD) δ ppm 8.21 (m, 1H), 7.95 (m, 1H), 7.83 (m, 1H), 7.59 (m, 2H), 7.53 (m, 1H), 7.23 (m, 2H), 5.55 (d, J = 1.8 Hz, 1H), 4.03 (dd, J = 1.8, 3.3 Hz, 1H), 3.91−3.96 (m, 4H), 3.70−3.82 (m, 3H), 3.59−3.65 (m, 1H). MS (ESI): found $[M + H]^+$, 391.1.

(2*R*,3*S*,4*S*,5*S*,6*R*)-2-(Hydroxymethyl)-6-(3-nitrophenoxy)tetrahydropyran-3,4,5-triol (3c). 3c was prepared using the same procedure as for **8e**. Yield: 46%. ^{1}H NMR (300 MHz, methanol-d_4) δ ppm 3.51−3.60 (m, 1 H), 3.67−3.81 (m, 3 H), 3.87−3.95 (m, 1 H), 4.05 (dd, J = 3.30, 1.65 Hz, 1 H), 5.61 (d, J = 1.65 Hz, 1 H), 7.50−7.60 (m, 2 H), 7.85−7.94 (m, 1 H), 7.97 (dt, J = 2.75, 1.10 Hz, 1 H). MS (ESI): found $[2M + H]^+$, 603.1.

(2*R*,3*S*,4*S*,5*S*,6*R*)-2-(Hydroxymethyl)-6-(3-methylphenoxy)tetrahydropyran-3,4,5-triol (3e). 3e was prepared using the same procedure as for **8e**. Yield: 27%. ^{1}H NMR (300 MHz, methanol-d_4) δ ppm 2.30 (s, 3 H), 3.56−3.66 (m, 1 H), 3.68−3.82 (m, 3 H), 3.87−3.95 (m, 1 H), 3.99 (dd, J = 3.43, 1.79 Hz, 1 H), 5.45 (d, J = 1.92 Hz, 1 H), 6.79−7.00 (m, 3 H), 7.14 (t, J = 7.83 Hz, 1 H). MS (ESI): found $[2M + H]^+$, 540.9.

(2*R*,3*S*,4*S*,5*S*,6*R*)-2-(Hydroxymethyl)-6-(4-methylphenoxy)tetrahydropyran-3,4,5-triol (3f). 3f was prepared using the same procedure as for **8e**. Yield: 44%. ^{1}H NMR (300 MHz, methanol-d_4) δ ppm 2.26 (s, 3 H), 3.57−3.66 (m, 1 H), 3.68−3.82 (m, 3 H), 3.86−3.95 (m, 1 H), 3.99 (dd, J = 3.30, 1.92 Hz, 1 H), 5.41 (d, J = 1.92 Hz, 1 H), 6.95−7.04 (m, 2 H), 7.05−7.13 (m, 2 H). MS (ESI): found $[2M + H]^+$, 541.4.

(2*R*,3*S*,4*S*,5*S*,6*R*)-2-(2-Chlorophenoxy)-6-(hydroxymethyl)tetrahydropyran-3,4,5-triol (3g). 3g was prepared using the same procedure as for **8e**. Yield: 29%. ^{1}H NMR (300 MHz, methanol-d_4) δ ppm 3.60−3.69 (m, 1 H), 3.70−3.81 (m, 3 H), 3.98 (dd, J = 9.20, 3.43 Hz, 1 H), 4.10 (dd, J = 3.30, 1.92 Hz, 1 H), 5.53 (d, J = 1.65 Hz, 1 H), 7.00 (td, J = 7.69, 1.37 Hz, 1 H), 7.25 (ddd, J = 8.24, 7.42, 1.65 Hz, 1 H), 7.32−7.41 (m, 2 H). MS (ESI): found $[M + Na]^+$, 312.7.

(2*R*,3*S*,4*S*,5*S*,6*R*)-2-(3-Chlorophenoxy)-6-(hydroxymethyl)tetrahydropyran-3,4,5-triol (3h). 3h was prepared using the same procedure as for **8e**. Yield: 58%. ^{1}H NMR (300 MHz, methanol-d_4) δ ppm 3.51−3.61 (m, 1 H), 3.67−3.81 (m, 3 H), 3.84−3.92 (m, 1 H), 4.00 (dd, J = 2.88, 2.06 Hz, 1 H), 5.48 (d, J = 1.65 Hz, 1 H), 6.97−7.09 (m, 2 H), 7.12−7.18 (m, 1 H), 7.21−7.30 (m, 1 H). MS (ESI): found $[M + K]^+$, 328.6.

(2*R*,3*S*,4*S*,5*S*,6*R*)-2-(4-Chlorophenoxy)-6-(hydroxymethyl)tetrahydropyran-3,4,5-triol (3i). 3i was prepared using the same procedure as for **8e**. Yield: 65%. ^{1}H NMR (300 MHz, methanol-d_4) δ ppm 3.52−3.62 (m, 1 H), 3.66−3.81 (m, 3 H), 3.83−3.91 (m, 1 H), 3.99 (dd, J = 3.43, 1.79 Hz, 1 H), 5.45 (d, J = 1.65 Hz, 1 H), 7.06−7.17 (m, 2 H), 7.22−7.32 (m, 2 H). MS (ESI): found $[2M + Na]^+$, 603.0.

Methyl 3-[(2*R*,3*S*,4*S*,5*S*,6*R*)-3,4,5-Trihydroxy-6-(hydroxymethyl)tetrahydropyran-2-yl]oxybenzoate (3j). 3j was prepared using the same procedure as for **8e**. Yield: 75%. ^{1}H NMR (300 MHz, methanol-d_4) δ ppm 3.52−3.64 (m, 1 H), 3.65−3.82 (m, 3 H), 3.84−3.98 (m, 4 H), 4.02 (dd, J = 3.30, 1.92 Hz, 1 H), 5.54 (d, J = 1.65 Hz, 1 H), 7.31−7.51 (m, 2 H), 7.62−7.81 (m, 2 H). MS (ESI): found $[M + Na]^+$, 336.8.

Methyl 4-[(2*R*,3*S*,4*S*,5*S*,6*R*)-3,4,5-Trihydroxy-6-(hydroxymethyl)tetrahydropyran-2-yl]oxybenzoate (3k). 3k was prepared using the same procedure as for **8e**. Yield: 60%. ^{1}H NMR (300 MHz, deuterium oxide) δ ppm 3.61−3.69 (m, 1 H), 3.70−3.80 (m, 3 H), 3.90 (s, 3 H), 4.06 (dd, J = 3.60, 9.30 Hz, 1 H), 4.17 (dd, J = 3.30, 1.80 Hz, 1 H), 5.72 (d, J = 1.80 Hz, 1 H), 7.20−7.26 (m, 2 H), 7.98 − 8.04 (m, 2 H). MS (ESI): found $[M + Na]^+$, 337.4.

2-[(2*R*,3*S*,4*S*,5*S*,6*R*)-3,4,5-Trihydroxy-6-(hydroxymethyl)tetrahydropyran-2-yl]oxybenzonitrile (3m). 3m was prepared using the same procedure as for **8e** and was further purified by silica gel chromatography with methylene chloride and methanol combination as eluent. Yield: 55%. ^{1}H NMR (300 MHz, methanol-d_4) δ ppm 3.51−3.63 (m, 1 H), 3.65−3.85 (m, 3 H), 3.98 (dd, J = 9.48, 3.43 Hz, 1 H), 4.10 (dd, J = 3.30, 1.92 Hz, 1 H), 5.66 (d, J = 1.65 Hz, 1 H), 7.15 (td, J = 7.55, 1.10 Hz, 1 H), 7.48 (d, J = 8.24 Hz, 1 H), 7.56−7.70 (m, 2 H). MS (ESI): found $[M + H]^+$, 281.8.

3-[(2*R*,3*S*,4*S*,5*S*,6*R*)-3,4,5-Trihydroxy-6-(hydroxymethyl)tetrahydropyran-2-yl]oxybenzonitrile (3n). 3n was prepared using the same procedure as for **8e**. Yield: 64%. ^{1}H NMR (300 MHz, methanol-d_4) δ ppm 3.48−3.60 (m, 1 H), 3.63−3.82 (m, 3 H), 3.89 (dd, J = 9.48, 3.43 Hz, 1 H), 4.02 (dd, J = 3.30, 1.92 Hz, 1 H), 5.55 (d, J = 1.37 Hz, 1 H), 7.30−7.57 (m, 4 H). MS (ESI): found $[M + K]^+$, 320.1.

4-[(2*R*,3*S*,4*S*,5*S*,6*R*)-3,4,5-Trihydroxy-6-(hydroxymethyl)tetrahydropyran-2-yl]oxybenzonitrile (3o). 3o was prepared using the same procedure as for **8e**. Yield: 33%. ^{1}H NMR (300 MHz, methanol-d_4) δ ppm 3.44−3.60 (m, 1 H), 3.60−3.82 (m, 3 H), 3.88 (dd, J = 9.34, 3.30 Hz, 1 H), 3.96−4.19 (m, 1 H), 5.48−5.74 (m, 1 H), 7.27 (d, J = 8.79 Hz, 2 H), 7.68 (d, J = 8.79 Hz, 2 H). MS (ESI): found $[2M + Na]^+$, 585.8.

(2*R*,3*S*,4*S*,5*S*,6*R*)-2-(Hydroxymethyl)-6-(4-methoxyphenoxy)tetrahydropyran-3,4,5-triol (3p). 3p was prepared using the same procedure as for **8e**. Yield: 56%. ^{1}H NMR (300 MHz, methanol-d_4) δ ppm 3.61−3.68 (m, 1 H), 3.69−3.83 (m, 6 H), 3.85−3.92 (m, 1 H), 3.99 (dd, J = 3.30, 1.92 Hz, 1 H), 5.34 (d, J = 1.92 Hz, 1 H), 6.78−6.91 (m, 2 H), 6.96−7.12 (m, 2 H). MS (ESI): found $[M + Na]^+$, 308.7.

***N*-[2-[(2*R*,3*S*,4*S*,5*S*,6*R*)-3,4,5-Trihydroxy-6-(hydroxymethyl)tetrahydropyran-2-yl]oxyphenyl]acetamide (3q). 3q** was prepared using the same procedure as for **8e**. Yield: 42%. ^{1}H NMR (300 MHz, methanol-d_4) δ ppm 2.17 (s, 3 H), 3.56−3.67 (m, 1 H), 3.67−3.83 (m, 3 H), 3.93 (dd, J = 9.07, 3.30 Hz, 1 H), 4.09 (br. s., 1 H), 5.46 (s, 1 H), 6.92−7.07 (m, 1 H), 7.15 (t, J = 7.14 Hz, 1 H), 7.34 (d, J = 7.97 Hz, 1 H), 7.53−7.75 (m, 1 H). MS (ESI): found $[M + Na]^+$, 335.9.

***N*-[3-[(2*R*,3*S*,4*S*,5*S*,6*R*)-3,4,5-Trihydroxy-6-(hydroxymethyl)tetrahydropyran-2-yl]oxyphenyl]acetamide (3r). 3r** was prepared using the same procedure as for **8e**. Yield: 79%. ^{1}H NMR (300 MHz, methanol-d_4) δ ppm 2.11 (s, 3 H), 3.54−3.65 (m, 1 H), 3.67−3.82 (m, 3 H), 3.86−3.95 (m, 1 H), 4.00 (dd, J = 3.30, 1.92 Hz, 1 H), 5.47 (d, J = 1.37 Hz, 1 H), 6.79−6.96 (m, 1 H), 7.05−7.31 (m, 2 H), 7.43 (t, J = 2.06 Hz, 1 H). MS (ESI): found $[M + H]^+$, 314.3.

***N*-[4-[(2*R*,3*S*,4*S*,5*S*,6*R*)-3,4,5-Trihydroxy-6-(hydroxymethyl)tetrahydropyran-2-yl]oxyphenyl]acetamide (3s). 3s** was prepared using the same procedure as for **8e**. Yield: 38%. ^{1}H NMR (300 MHz, methanol-d_4) δ ppm 2.10 (s, 3 H), 3.53−3.65 (m, 1 H), 3.67−3.82 (m, 3 H), 3.83−3.94 (m, 1 H), 3.99 (dd, J = 3.43, 1.79 Hz, 1 H), 5.42 (d, J = 1.65 Hz, 1 H), 6.98−7.18 (m, 2 H), 7.36−7.57 (m, 2 H). MS (ESI): found $[M + H]^+$, 313.7.

3-[(2*R*,3*S*,4*S*,5*S*,6*R*)-3,4,5-Trihydroxy-6-(hydroxymethyl)tetrahydropyran-2-yl]oxybenzamide (3t). 3t was prepared using the same procedure as for **8e**. Yield: 24%. ^{1}H NMR (300 MHz, methanol-d_4) δ ppm 3.55−3.64 (m, 1 H), 3.65−3.82 (m, 3 H), 3.87−3.95 (m, 1 H), 4.03 (dd, J = 3.30, 1.92 Hz, 1 H), 5.55 (d, J = 1.92 Hz, 1 H), 7.26−7.33 (m, 1 H), 7.39 (t, J = 7.83 Hz, 1 H), 7.53 (dt, J = 7.55, 1.17 Hz, 1 H), 7.58−7.65 (m, 1 H). MS (ESI): found $[2M + H]^+$, 597.9.

4-[(2*R*,3*S*,4*S*,5*S*,6*R*)-3,4,5-Trihydroxy-6-(hydroxymethyl)tetrahydropyran-2-yl]oxybenzamide (3u). 3u was prepared using the same procedure as for **8e**. Yield: 38%. ^{1}H NMR (300 MHz,

methanol-d_4) δ ppm 3.49−3.60 (m, 1 H), 3.65−3.81 (m, 3 H), 3.86−3.94 (m, 1 H), 4.02 (dd, J = 3.43, 1.79 Hz, 1 H), 5.57 (d, J = 1.65 Hz, 1 H), 7.12−7.28 (m, 2 H), 7.79−7.93 (m, 2 H). MS (ESI): found $[M + H]^+$, 300.9.

Methyl 2-[4-[(2*R*,3*S*,4*S*,5*S*,6*R*)-3,4,5-Trihydroxy-6-(hydroxymethyl)tetrahydropyran-2-yl]oxyphenyl]acetate (3w). 3w was prepared using the same procedure as for **8e**. Yield: 74%. ^{1}H NMR (300 MHz, methanol-d_4) δ ppm 3.54−3.64 (m, 3 H), 3.65−3.82 (m, 6 H), 3.86−3.94 (m, 1 H), 3.99 (dd, J = 3.30, 1.92 Hz, 1 H), 5.45 (d, J = 1.65 Hz, 1 H), 6.98−7.14 (m, 2 H), 7.20 (d, J = 8.79 Hz, 2 H). MS (ESI): found $[M + H]^+$, 328.5.

Dimethyl 5-[(2*R*,3*S*,4*S*,5*S*,6*R*)-3,4,5-Trihydroxy-6-(hydroxymethyl)tetrahydropyran-2-yl]oxybenzene-1,3-dicarboxylate (4). 4 was prepared using the same procedure as for **8e**. Yield: 75%. ^{1}H NMR (300 MHz, methanol-d_4) δ ppm 3.49−3.62 (m, 1 H), 3.66−3.85 (m, 3 H), 3.86−4.01 (m, 7 H), 4.02−4.11 (m, 1 H), 5.62 (s, 1 H), 7.94 (d, J = 1.10 Hz, 2 H), 8.27 (s, 1 H). MS (ESI): found $[M + H]^+$, 373.0.

(2*R*,3*S*,4*S*,5*S*,6*R*)-2-Benzyloxy-6-(hydroxymethyl)tetrahydropyran-3,4,5-triol (5a). 5a was prepared using the same procedure as for **8e**. Yield: 52%. ^{1}H NMR (300 MHz, deuterium oxide) δ ppm 3.59−3.88 (m, 5 H), 3.92 (dd, J = 3.30, 1.65 Hz, 1 H), 4.55 (d, J = 11.54 Hz, 1 H), 4.75 (d, J = 11.54 Hz, 1 H), 4.95 (d, J = 1.65 Hz, 1 H), 7.28−7.56 (m, 5 H). MS (ESI): found $[M + Na]^+$, 293.0.

(2*R*,3*S*,4*S*,5*S*,6*R*)-2-(Hydroxymethyl)-6-[(4-nitrophenyl)methoxy]tetrahydropyran-3,4,5-triol (5b). 5b was prepared using the same procedure as for **8e**. Yield: 76%. ^{1}H NMR (300 MHz, methanol-d_4) δ ppm 3.53−3.65 (m, 2 H), 3.65−3.80 (m, 2 H), 3.82−3.88 (m, 1 H), 3.89 (dd, J = 3.43, 1.79 Hz, 1 H), 4.67 (d, J = 13.19 Hz, 1 H), 4.92 (d, J = 13.19 Hz, 1 H), 7.60−7.65 (m, 2 H), 8.15−8.33 (m, 2 H). MS (ESI): found $[M + Na]^+$, 337.6.

(2*R*,3*S*,4*S*,5*S*,6*R*)-2-(Hydroxymethyl)-6-(2-naphthyloxy)tetrahydropyran-3,4,5-triol (7b). 7b was prepared using the same procedure as for **8e**. Yield: 50%. ^{1}H NMR (300 MHz, methanol-d_4) δ ppm 3.60−3.69 (m, 1 H), 3.70−3.87 (m, 3 H), 3.97 (dd, J = 9.34, 3.57 Hz, 1 H), 4.07 (dd, J = 3.43, 1.79 Hz, 1 H), 5.63 (d, J = 1.65 Hz, 1 H), 7.24 (dd, J = 8.79, 2.47 Hz, 1 H), 7.30−7.38 (m, 1 H), 7.39−7.48 (m, 1 H), 7.57 (d, J = 2.47 Hz, 1 H), 7.71−7.90 (m, 3 H). MS (ESI): found $[M + H]^+$, 307.0.

6-[(2*R*,3*S*,4*S*,5*S*,6*R*)-3,4,5-Trihydroxy-6-(hydroxymethyl)tetrahydropyran-2-yl]oxy-3a,7a-dihydro-3*H*-1,3-benzoxazol-2-one (7c). 7c was prepared using the same procedure as for **8e** and was further purified by silica gel chromatography with methylene chloride and methanol combination as eluent. Yield: 32%. ^{1}H NMR (300 MHz, methanol-d_4) δ ppm 3.59−3.67 (m, 1 H), 3.67−3.83 (m, 3 H), 3.84−3.91 (m, 1 H), 4.01 (dd, J = 3.30, 1.92 Hz, 1 H), 5.40 (d, J = 1.65 Hz, 1 H), 6.89−7.04 (m, 2 H), 7.13 (d, J = 2.20 Hz, 1 H). MS (ESI): found $[M + Na]^+$, 336.0.

Methyl 5-[(2*R*,3*S*,4*S*,5*S*,6*R*)-3,4,5-Trihydroxy-6-(hydroxymethyl)-tetrahydropyran-2-yl]oxybenzothiophene-2-carboxylate (7d). 7d was prepared using the same procedure as for **8e**. Yield: 66%. ^{1}H NMR (300 MHz, methanol-d_4) δ ppm 3.59−3.67 (m, 1 H), 3.68−3.84 (m, 3 H), 3.89−3.97 (m, 4 H), 4.05 (dd, J = 3.30, 1.92 Hz, 1 H), 5.55 (d, J = 1.65 Hz, 1 H), 7.27 (dd, J = 8.79, 2.47 Hz, 1 H), 7.72 (d, J = 2.47 Hz, 1 H), 7.81 (d, J = 8.79 Hz, 1 H), 8.01 (s, 1 H). MS (ESI): found $[M + H]^+$, 371.6.

Methyl 6-[(2*R*,3*S*,4*S*,5*S*,6*R*)-3,4,5-Trihydroxy-6-(hydroxymethyl)tetrahydropyran-2-yl]oxybenzothiophene-2-carboxylate (7e). 7e was prepared using the same procedure as for **8e**. Yield: 50%. ^{1}H NMR (300 MHz, methanol-d_4) δ ppm 3.55−3.64 (m, 1 H), 3.67−3.81 (m, 3 H), 3.84−3.98 (m, 4 H), 4.05 (dd, J = 3.43, 1.79 Hz, 1 H), 5.58 (d, J = 1.65 Hz, 1 H), 7.19 (dd, J = 8.79, 2.20 Hz, 1 H), 7.74 (d, J = 2.20 Hz, 1 H), 7.85 (d, J = 8.79 Hz, 1 H), 8.02 (s, 1 H). MS (ESI): found $[M + H]^+$, 371.5.

(2*R*,3*S*,4*S*,5*S*,6*R*)-2-(Hydroxymethyl)-6-(2-phenylphenoxy)-tetrahydropyran-3,4,5-triol (8a). 8a was prepared using the same procedure as for **8e** and was further purified by HPLC (C18, 15 mm × 150 mm column; eluent acetonitrile/water (0.1% TFA)). Yield: 60%. Purity: 85%. ^{1}H NMR (300 MHz, methanol-d_4) δ ppm 3.54 (td, J = 4.74, 2.88 Hz, 1 H), 3.63−3.78 (m, 4 H), 3.82 (t, J = 2.20 Hz, 1 H), 5.40 (d, J = 1.92 Hz, 1 H), 7.06−7.15 (m, 1 H), 7.26−7.35 (m, 3 H), 7.35−7.44 (m, 3 H), 7.44−7.51 (m, 2 H). MS (ESI): found $[2M + H]^+$, 665.1.

Methyl 4-[3-[(2*R*,3*S*,4*S*,5*S*,6*R*)-3,4,5-Trihydroxy-6-(hydroxymethyl)tetrahydropyran-2-yl]oxyphenyl]benzoate (8b). 8b was prepared using the same procedure as for **8e**. Yield: 77%. ^{1}H NMR (300 MHz, methanol-d_4) δ ppm 3.60−3.84 (m, 4 H), 3.86−3.98 (m, 4 H), 4.04 (dd, J = 3.43, 1.79 Hz, 1 H), 5.56 (d, J = 1.92 Hz, 1 H), 7.17 (ddd, J = 8.04, 2.40, 1.10 Hz, 1 H), 7.28−7.54 (m, 3 H), 7.66−7.85 (m, 2 H), 8.00−8.22 (m, 2 H). MS (ESI): found $[M + H]^+$, 391.6.

(2*R*,3*S*,4*S*,5*S*,6*R*)-2-(Hydroxymethyl)-6-(4-phenylphenoxy)-tetrahydropyran-3,4,5-triol (8c). 8c was prepared using the same procedure as for **8e**. Yield: 73%. ^{1}H NMR (300 MHz, methanol-d_4) δ ppm 3.57−3.67 (m, 1 H), 3.69−3.84 (m, 3 H), 3.87−3.97 (m, 1 H), 4.03 (dd, J = 3.57, 1.92 Hz, 1 H), 5.53 (d, J = 1.92 Hz, 1 H), 7.15−7.23 (m, 2 H), 7.24−7.32 (m, 1 H), 7.35−7.45 (m, 2 H), 7.49−7.60 (m, 4 H). MS (ESI): found $[2M + H]^+$, 664.9.

Phenyl-[3-[(2*R*,3*S*,4*S*,5*S*,6*R*)-3,4,5-trihydroxy-6-(hydroxymethyl)-tetrahydropyran-2-yl]oxyphenyl]methanone (8d). 8d was prepared using the same procedure as for **8e**. Yield: 83%. ^{1}H NMR (300 MHz, methanol-d_4) δ ppm 3.56−3.66 (m, 1 H), 3.70−3.85 (m, 3 H), 3.88−3.98 (m, 1 H), 4.05 (dd, J = 3.43, 1.79 Hz, 1 H), 5.56 (d, J = 1.65 Hz, 1 H), 7.33−7.46 (m, 3 H), 7.46−7.57 (m, 3 H), 7.57−7.67 (m, 1 H), 7.70−7.83 (m, 2 H). MS (ESI): found $[M + H]^+$, 361.1.

Methyl 4-[4-[(2*R*,3*S*,4*S*,5*S*,6*R*)-3,4,5-Trihydroxy-6-(hydroxymethyl)tetrahydropyran-2-yl]oxyphenyl]benzoate (8f). 8f was prepared using the same procedure as for **8e**. Yield: 40%. ^{1}H NMR (300 MHz, methanol-d_4/chloroform-d_1) δ ppm 3.56−3.69 (m, 1 H), 3.71−3.86 (m, 3 H), 3.88−3.99 (m, 4 H), 4.04 (dd, J = 3.30, 1.92 Hz, 1 H), 5.54 (d, J = 1.65 Hz, 1 H), 7.03−7.23 (m, 2 H), 7.53−7.58 (m, 2 H), 7.62 (d, J = 8.52 Hz, 2 H), 8.04 (d, J = 8.52 Hz, 2 H). MS (ESI): found $[M + K]^+$, 429.5.

***N*-[3-[4-[(2*R*,3*S*,4*S*,5*S*,6*R*)-3,4,5-Trihydroxy-6-(hydroxymethyl)-tetrahydropyran-2-yl]oxyphenyl]phenyl]acetamide (14b). 14b** was prepared using the same procedure as for **8e**. Yield: 50%. ^{1}H NMR (300 MHz, methanol-d_4) δ ppm 2.14 (s, 3 H), 3.63 (ddd, J = 7.28, 4.94, 2.33 Hz, 1 H), 3.68−3.84 (m, 3 H), 3.88−3.98 (m, 1 H), 4.04 (dd, J = 3.43, 1.79 Hz, 1 H), 5.53 (d, J = 1.65 Hz, 1 H), 7.09−7.23 (m, 2 H), 7.24−7.39 (m, 2 H), 7.41−7.62 (m, 3 H), 7.78 (t, J = 1.65 Hz, 1 H). MS (ESI): found $[M + H]^+$, 390.2.

Dimethyl 5-[4-[(2*R*,3*S*,4*S*,5*S*,6*R*)-3,4,5-Trihydroxy-6-(hydroxymethyl)tetrahydropyran-2-yl]oxyphenyl]benzene-1,3-dicarboxylate (15a). 15a was prepared using the same procedure as for **8e** and was further purified by silica gel chromatography with chloroform and methanol combination as eluent. Yield: 53%. ^{1}H NMR (300 MHz, methanol-d_4) δ ppm 3.57−3.66 (m, 1 H), 3.68−3.84 (m, 3 H), 3.93 (dd, J = 9.34, 3.30 Hz, 1 H), 3.97 (s, 6 H), 4.04 (dd, J = 3.30, 1.92 Hz, 1 H), 5.56 (d, J = 1.65 Hz, 1 H), 7.21−7.36 (m, 2 H), 7.59−7.72 (m, 2 H), 8.42 (d, J = 1.65 Hz, 2 H), 8.55 (t, J = 1.51 Hz, 1 H). MS (ESI): found $[M + H]^+$, 449.6.

Procedure for the Preparation of Mannosides Using 2,3,4,6-Tetra-*O*-benzyl-1-acetyl-α-D-mannopyranose:[3] **[3-[(2*R*,3*S*,4*S*,5*S*,6*R*)-3,4,5-Trihydroxy-6-(hydroxymethyl)tetrahydropyran-2-yl]oxyphenyl]acetate (3v). [3-[(2*R*,3*S*,4*S*,5*R*,6*R*)-3,4,5-Tribenzyloxy-6-(benzyloxymethyl)tetrahydropyran-2-yl]oxyphenyl]acetate.** Under nitrogen atmosphere, at 0 °C boron trifluoride diethyl etherate (0.051 g, 0.36 mmol) was added dropwise into the solution of 2,3,4,6-tetra-*O*-benzyl-1-acetyl-α-D-mannopyranose (0.106 g, 0.18 mmol) and resorcinol monoacetate (0.055 g, 0.36 mmol) in 7 mL of CH_2Cl_2. The mixture was stirred at 0 °C and monitored by TLC. The reaction was then quenched with water and extracted with CH_2Cl_2. The CH_2Cl_2 layer was collected, dried with Na_2SO_4, and concentrated in vacuo. The resulting residue was purified by silica gel chromography with hexane/ethyl acetate combinations as eluent to give [3-[(2*R*,3*S*,4*S*,5*R*,6*R*)-3,4,5-tribenzyloxy-6-(benzyloxymethyl)-tetrahydropyran-2-yl]oxyphenyl]acetate (0.093 g) in 75% yield. ^{1}H NMR (300 MHz, $CDCl_3$) δ ppm 7.15−7.40 (m, 21H), 6.88−6.91

(m, 1H), 6.81(t, J = 2.4 Hz, 1H), 6.73−6.76 (m, 1H), 5.58 (d, J = 1.8 Hz, 1H), 4.90 (d, J = 10.8 Hz, 1H), 4.78 (s, 2H), 4.64−4.69 (m, 3H), 4.52 (d, J = 10.8 Hz, 1H), 4.45 (d, J = 12.3 Hz, 1H), 4.05−4.18 (m, 2H), 3.94 (t, J = 2.4 Hz, 1H), 3.77−3.85 (m, 2H), 3.64−3.70 (m, 1H), 2.27 (s, 3H). MS (ESI): found $[M + Na]^+$, 697.2.

[3-[(2*R*,3*S*,4*S*,5*S*,6*R*)-3,4,5-Trihydroxy-6-(hydroxymethyl)-tetrahydropyran-2-yl]oxyphenyl]acetate (3v). Under hydrogen atmosphere [3-[3,4,5-tribenzyloxy-6-(benzyloxymethyl)tetrahydropyran-2-yl]oxyphenyl]acetate (0.085 g, 0.13 mmol) was stirred with Pd/C(10 wt %) (0.132 g, 0.063 mmol) in ethanol (6 mL) and ethyl acetate (6 mL). The reaction was monitored by TLC until it went into completion. The mixture was filtered through a Celite plug. The filtrate was concentrated and then dried in vacuo, furnishing pure **3v** (0.040 g) in quantitative yield. ^{1}H NMR (300 MHz, CD_3OD) δ ppm 7.30 (t, J = 8.1 Hz, 1H), 7.00 (m, 1H), 6.90 (t, J = 2.1 Hz, 1H), 6.76 (m, 1H), 5.47 (d, J = 1.8 Hz, 1H), 4.00 (dd, J = 1.8, 3.3 Hz, 1H), 3.88 (dd, J = 3.3, 9.3 Hz, 1H), 3.68−3.79 (m, 3H), 3.54−3.61 (m, 1H). MS (ESI): found $[M + H]^+$, 314.9.

5-[(2*R*,3*S*,4*S*,5*S*,6*R*)-3,4,5-Trihydroxy-6-(hydroxymethyl)-tetrahydropyran-2-yl]oxy-3*H*-benzofuran-2-one (7a). 7a prepared in the same way as **3v**. Yield: 59%. Purity: 91%. ^{1}H NMR (300 MHz, D_2O) δ ppm 7.19 (m, 1H), 7.11 (m, 2H), 5.52 (d, J = 1.5 Hz, 1H), 4.15−4.18 (m, 1H), 3.97−4.05 (m, 1H), 3.68−3.88 (m, 6H). MS (ESI): found $[M + H]^+$, 313.0.

Procedure for the Preparation of Glucoside Analogues: Methyl 3-[4-[(2*R*,3*R*,4*S*,5*S*,6*R*)-3,4,5-Trihydroxy-6-(hydroxymethyl)-tetrahydropyran-2-yl]oxyphenyl]benzoate (α-Anomer, 11a) and Methyl 3-[4-[(2*S*,3*R*,4*S*,5*S*,6*R*)-3,4,5-Trihydroxy-6-(hydroxymethyl)-tetrahydropyran-2-yl]oxyphenyl]benzoate (*β*-Anomer, 11b). Methyl 3-[4-[(2*R*,3*R*,4*S*,5*R*,6*R*)-3,4,5-Tribenzoyloxy-6-(benzoyloxymethyl)-tetrahydropyran-2-yl]oxyphenyl]benzoate (α-Anomer) and Methyl 3-[4-[(2*S*,3*R*,4*S*,5*R*,6*R*)-3,4,5-Tribenzoyloxy-6-(benzoyloxymethyl)-tetrahydropyran-2-yl]oxyphenyl]benzoate (*β*-Anomer). Under nitrogen atmosphere, at 0 °C boron trifluoride diethyl etherate (0.212 g, 1.5 mmol) was added dropwise into a solution of glucose pentabenzoate **9** (0.350 g, 0.5 mmol) and methyl 3-(4-hydroxyphenyl)benzoate **10** (0.228 g, 1.0 mmol) in 10 mL of CH_2Cl_2. After a few minutes the mixture was heated to reflux and was kept stirring for more than 36 h. The reaction was then quenched with water and extracted with CH_2Cl_2. The CH_2Cl_2 layer was collected, dried with Na_2SO_4, then concentrated in vacuo. The residue was purified by HPLC (C18, 15 mm × 150 mm column; eluent acetonitrile/water (0.1% TFA)) to give benzoyl-protected glucosides, methyl 3-[4-[(2*R*,3*R*,4*S*,5*R*,6*R*)-3,4,5-tribenzoyloxy-6-(benzoyloxymethyl)-tetrahydropyran-2-yl]oxyphenyl]benzoate (α-anomer) (0.026 g) and methyl 3-[4-[(2*S*,3*R*,4*S*,5*R*,6*R*)-3,4,5-tribenzoyloxy-6-(benzoyloxymethyl)tetrahydropyran-2-yl]oxyphenyl]benzoate (*β*-anomer) (0.045 g) totally in 18% yield. Benzoyl-protected glucoside α-anomer: ^{1}H NMR (300 MHz, acetonitrile-d_3) δ ppm 3.86−3.94 (m, 3 H), 4.44−4.56 (m, 2 H), 4.64−4.75 (m, 1 H), 5.66 (dd, J = 10.16, 3.57 Hz, 1 H), 5.79 (t, J = 9.89 Hz, 1 H), 6.12 (d, J = 3.85 Hz, 1 H), 6.32 (t, J = 9.89 Hz, 1 H), 7.27−7.33 (m, 2 H), 7.34−7.47 (m, 8 H), 7.49−7.63 (m, 7 H), 7.77 (ddd, J = 7.69, 1.92, 1.10 Hz, 1 H), 7.83−7.89 (m, 2 H), 7.90−7.99 (m, 7 H), 8.11−8.19 (m, 1 H). MS (ESI): found $[M + Na]^+$, 829.5. Benzoyl-protected glucoside *β*-anomer: ^{1}H NMR (300 MHz, acetonitrile-d_3) δ ppm 3.91 (s, 3 H), 4.50−4.69 (m, 3 H), 5.68−5.88 (m, 3 H), 5.98−6.14 (t, J = 9.6 Hz, 1 H), 7.06−7.17 (m, 2 H), 7.32−7.70 (m, 15 H), 7.73−7.87 (m, 3 H), 7.88−8.01 (m, 5 H), 8.02−8.11 (m, 2 H), 8.14 (t, J = 1.79 Hz, 1 H). MS (ESI): found $[M + Na]^+$, 829.8.

Methyl 3-[4-[(2*R*,3*R*,4*S*,5*S*,6*R*)-3,4,5-Trihydroxy-6-(hydroxymethyl)tetrahydropyran-2-yl]oxyphenyl]benzoate (α-Anomer, 11a) and Methyl 3-[4-[(2*S*,3*R*,4*S*,5*S*,6*R*)-3,4,5-Trihydroxy-6-(hydroxymethyl)tetrahydropyran-2-yl]oxyphenyl]benzoate (*β*-Anomer, 11b). Deprotection of the benzoyl-protected glucoside α-anomer and benzoyl-protected glucoside *β*-anomer with a catalytic amount of sodium methoxide in methanol was done in the same way as for **8e**, and subsequent purification by HPLC (C18, 15 mm × 150 mm column; eluent acetonitrile/water (0.1% TFA)) furnished glucosides α-anomer **11a** (0.009 g) and *β*-anomer **11b** (0.016 g) in 71% yield. Glucoside α-anomer **11a**: ^{1}H NMR (300 MHz, methanol-d_4) δ ppm 3.40−3.50 (m, 1 H), 3.56−3.63 (m, 1 H), 3.64−3.81 (m, 3 H), 3.89 (dd, J = 9.75, 8.93 Hz, 1 H), 3.94 (s, 3 H), 5.55 (d, J = 3.57 Hz, 1 H), 7.23−7.36 (m, 2 H), 7.48−7.69 (m, 3 H), 7.83 (ddd, J = 7.83, 1.92, 1.24 Hz, 1 H), 7.96 (dt, J = 7.76, 1.48 Hz, 1 H), 8.21 (t, J = 1.65 Hz, 1 H). MS (ESI): found $[M + H]^+$, 391.4. Glucoside *β*-anomer **11b**: ^{1}H NMR (300 MHz, methanol-d_4) δ ppm 3.36−3.56 (m, 4 H), 3.72 (dd, J = 11.95, 5.36 Hz, 1 H), 3.85−4.01 (m, 4 H), 4.93−5.04 (m, 1 H), 7.12−7.30 (m, 2 H), 7.45−7.65 (m, 3 H), 7.75−7.87 (m, 1 H), 7.96 (dq, J = 7.69, 0.92 Hz, 1 H), 8.15−8.27 (m, 1 H). MS (ESI): found $[M + H]^+$, 391.7.

General Procedure for the Preparation of Biphenylmannoside Derivatives through Suzuki Coupling Reaction: 3-[4-[(2*R*,3*S*,4*S*,5*S*,6*R*)-3,4,5-Trihydroxy-6-(hydroxymethyl)tetrahydropyran-2-yl]oxyphenyl]benzonitrile (14e). [(2*R*,3*S*,4*S*,5*R*,6*R*)-3,4,5-Triacetoxy-6-[4-(3-cyanophenyl)phenoxy]tetrahydropyran-2-yl]methyl Acetate. Under nitrogen atmosphere, a mixture of acetyl-protected 4-bromophenylmannoside **12** (0.101 g, 0.2 mmol), *m*-cyanophenylboronic acid (0.044 g, 0.3 mmol), cesium carbonate (0.196 g, 0.6 mmol), and tetrakis(triphenylphosphine)palladium (0.023 g, 0.02 mmol) in dioxane/water (5 mL/1 mL) was heated at 80 °C with stirring for 1 h. The solvent was removed and the resulting residue was purified by silica gel chromography with hexane/ethyl acetate combinations as eluent to give [3,4,5-triacetoxy-6-[4-(3-cyanophenyl)phenoxy]tetrahydropyran-2-yl]-methyl acetate (0.080 g) in 76% yield. ^{1}H NMR (300 MHz, $CDCl_3$) δ ppm 7.82 (t, J = 1.5 Hz, 1H), 7.76 (dt, J = 7.69, 1.65 Hz, 1H), 7.58−7.65 (m, 1H), 7.47−7.57 (m, 3H), 7.16−7.24 (m, 2H), 5.55−5.65 (m, 2H), 5.47 (dd, J = 3.57, 1.92 Hz, 1H), 5.39 (t, J = 9.9 Hz, 1H), 4.25−4.34 (m, 1H), 4.04−4.17 (m, 2H), 2.22 (s, 3H), 2.06 (s, 3H), 2.05 (s, 3H), 2.04 (s, 3H). MS (ESI): found $[M + Na]^+$, 548.7.

3-[4-[(2*R*,3*S*,4*S*,5*S*,6*R*)-3,4,5-Trihydroxy-6-(hydroxymethyl)-tetrahydropyran-2-yl]oxyphenyl]benzonitrile (14e). [3,4,5-Triacetoxy-6-[4-(3-cyanophenyl)phenoxy]tetrahydropyran-2-yl]methyl acetate (0.075 g) was stirred in 6 mL of methanol with a catalytic amount of sodium methoxide (0.02 M) at room temperature overnight. H^+ exchange resin (DOWEX 50WX4-100) was added to neutralize the mixture. The resin was filtered off and the filtrate was concentrated andthen dried in vacuo, giving rise to pure product **14e** (0.045 g) in 88% yield. ^{1}H NMR (300 MHz, CD_3OD) δ ppm 3.55−3.65 (m, 1H), 3.67−3.83 (m, 3H), 3.84−3.99 (m, 1H), 4.03 (dd, J = 3.43, 1.79 Hz, 1H), 5.55 (J = 1.65 Hz, 1H), 7.16−7.33 (m, 2H), 7.54−7.75 (m, 4H), 7.83−8.01 (m, 2H). MS (ESI): found $[M + H]^+$, 358.3.

(2*R*,3*S*,4*S*,5*S*,6*R*)-2-(Hydroxymethyl)-6-[4-(3-pyridyl)phenoxy]-tetrahydropyran-3,4,5-triol (8g). 8g was prepared using the same procedure as for **14e** except that H^+ exchange resin was not used. The product was further purified by silica gel chromatography with methylene chloride and methanol combination with 3% (v/v) ammonia aqueous as eluent. Yield: 65%. ^{1}H NMR (300 MHz, methanol-d_4) δ ppm 3.56−3.67 (m, 1 H), 3.68−3.85 (m, 3 H), 3.87−3.97 (m, 1 H), 4.04 (dd, J = 3.30, 1.92 Hz, 1 H), 5.56 (d, J = 1.92 Hz, 1 H), 7.21−7.32 (m, 2 H), 7.44−7.55 (m, 1 H), 7.56−7.69 (m, 2 H), 8.00−8.14 (m, 1 H), 8.47 (dd, J = 4.94, 1.37 Hz, 1 H), 8.72−8.82 (m, 1 H). MS (ESI): found $[M + H]^+$, 334.4.

(2*R*,3*S*,4*S*,5*S*,6*R*)-2-(Hydroxymethyl)-6-[4-(4-pyridyl)phenoxy]-tetrahydropyran-3,4,5-triol (8h). 8h was prepared using the same procedure as for **14e** except that H^+ exchange resin was not used. The product was further purified by silica gel chromatography with methylene chloride and methanol combination with 3% (v/v) ammonia aqueous as eluent. Yield: 12%. ^{1}H NMR (300 MHz, methanol-d_4) δ ppm 3.60 (ddd, J = 7.28, 4.94, 2.33 Hz, 1 H), 3.67−3.82 (m, 3 H), 3.87−3.97 (m, 1 H), 4.04 (dd, J = 3.43, 1.79 Hz, 1 H), 5.57 (d, J = 1.65 Hz, 1 H), 7.19−7.34 (m, 2 H), 7.61−7.82 (m, 4 H), 8.54 (d, J = 5.22 Hz, 2 H). MS (ESI): found $[M + H]^+$, 334.5.

2-[4-[(2*R*,3*S*,4*S*,5*S*,6*R*)-3,4,5-Trihydroxy-6-(hydroxymethyl)-tetrahydropyran-2-yl]oxyphenyl]benzonitrile (14d). 14d was prepared using the same procedure as for **14e**. Yield: 12%. It came from the minor product of the Suzuki coupling with 2-cyanophenylboronic acid. ^{1}H NMR (300 MHz, methanol-d_4) δ ppm 3.57−3.67 (m, 1 H), 3.69−3.85 (m, 3 H), 3.88−3.98 (m, 1 H), 4.04 (dd, J = 3.43, 1.79 Hz, 1 H), 5.57 (d, J = 1.65 Hz, 1 H), 7.21−7.32 (m, 2 H), 7.45−7.60 (m, 4 H), 7.66−7.76 (m, 1 H), 7.80 (dd, J = 7.69, 1.37 Hz, 1 H). MS (ESI): found $[M + H]^+$, 358.4.

4-[4-[(2*R*,3*S*,4*S*,5*S*,6*R*)-3,4,5-Trihydroxy-6-(hydroxymethyl)-tetrahydropyran-2-yl]oxyphenyl]benzonitrile (14f). 14f was prepared using the same procedure as for **14e**. Yield: 67%. ^{1}H NMR (300 MHz, methanol-d_4) δ ppm 3.52−3.67 (m, 1 H), 3.67−3.84 (m, 3 H), 3.87−3.98 (m, 1 H), 4.03 (dd, J = 3.43, 1.79 Hz, 1 H), 5.56 (d, J = 1.65 Hz, 1 H), 7.17−7.33 (m, 2 H), 7.56−7.70 (m, 2 H), 7.72−7.85 (m, 4 H). MS (ESI): found $[M + H]^+$, 358.3.

(2*R*,3*S*,4*S*,5*S*,6*R*)-2-(Hydroxymethyl)-6-[4-[2-(hydroxymethyl)-phenyl]phenoxy]tetrahydropyran-3,4,5-triol (14g). 14g was prepared using the same procedure as for **14e**. Yield: 79%. ^{1}H NMR (300 MHz, methanol-d_4) δ ppm 3.59−3.69 (m, 1 H), 3.70−3.83 (m, 3 H), 3.89−3.98 (m, 1 H), 4.04 (dd, J = 3.57, 1.92 Hz, 1 H), 4.51 (s, 2 H), 5.53 (d, J = 1.65 Hz, 1 H), 7.14−7.25 (m, 3 H), 7.27−7.43 (m, 4 H), 7.55 (dd, J = 7.55, 1.51 Hz, 1 H). MS (ESI): found $[M + Li]^+$, 365.4.

(2*R*,3*S*,4*S*,5*S*,6*R*)-2-(Hydroxymethyl)-6-[4-[3-(hydroxymethyl)-phenyl]phenoxy]tetrahydropyran-3,4,5-triol (14h). 14h was prepared using the same procedure as for **14e**. Yield: 70%. ^{1}H NMR (300 MHz, methanol-d_4) δ ppm 3.59−3.68 (m, 1 H), 3.69−3.84 (m, 3 H), 3.89−3.97 (m, 1 H), 4.03 (dd, J = 3.43, 1.79 Hz, 1 H), 4.66 (s, 2 H), 5.53 (d, J = 1.65 Hz, 1 H), 7.15−7.23 (m, 2 H), 7.26−7.33 (m, 1 H), 7.38 (t, J = 7.42 Hz, 1 H), 7.44−7.50 (m, 1 H), 7.52−7.61 (m, 3 H). MS (ESI): found $[M + Li]^+$, 365.5.

(2*R*,3*S*,4*S*,5*S*,6*R*)-2-(Hydroxymethyl)-6-[4-[4-(hydroxymethyl)-phenyl]phenoxy]tetrahydropyran-3,4,5-triol (14i). 14i was prepared using the same procedure as for **14e** and was further purified by HPLC (C18, 15 mm × 150 mm column; eluent acetonitrile/water (0.1% TFA)). Yield: 50%. ^{1}H NMR (300 MHz, methanol-d_4) δ ppm 3.58−3.69 (m, 1 H), 3.69−3.83 (m, 3 H), 3.89−3.98 (m, 1 H), 4.03 (dd, J = 3.30, 1.92 Hz, 1 H), 4.63 (s, 2 H), 5.52 (d, J = 1.65 Hz, 1 H), 7.14−7.28 (m, 2 H), 7.40 (d, J = 8.52 Hz, 2 H), 7.50−7.66 (m, 4 H). MS (ESI): found $[M + Li]^+$, 365.8.

(2*R*,3*S*,4*S*,5*S*,6*R*)-2-(Hydroxymethyl)-6-[4-(2-hydroxyphenyl)-phenoxy]tetrahydropyran-3,4,5-triol (14j). 14j was prepared using the same procedure as for **14e**. Yield: 74%. ^{1}H NMR (300 MHz, methanol-d_4) δ ppm 3.60−3.68 (m, 1 H), 3.69−3.84 (m, 3 H), 3.89−3.97 (m, 1 H), 4.03 (dd, J = 3.30, 1.92 Hz, 1 H), 5.52 (d, J = 1.65 Hz, 1 H), 6.83−6.92 (m, 2 H), 7.07−7.18 (m, 3 H), 7.19−7.25 (m, 1 H), 7.43−7.55 (m, 2 H). MS (ESI): found $[M + H]^+$, 349.4.

(2*R*,3*S*,4*S*,5*S*,6*R*)-2-(Hydroxymethyl)-6-[4-(3-hydroxyphenyl)-phenoxy]tetrahydropyran-3,4,5-triol (14k). 14k was prepared using the same procedure as for **14e**. Yield: 66%. ^{1}H NMR (300 MHz, methanol-d_4) δ ppm 3.56−3.67 (m, 1 H), 3.68−3.83 (m, 3 H), 3.88−3.96 (m, 1 H), 4.03 (dd, J = 3.43, 1.79 Hz, 1 H), 5.52 (d, J = 1.65 Hz, 1 H), 6.73 (ddd, J = 8.10, 2.33, 1.10 Hz, 1 H), 6.88−7.06 (m, 2 H), 7.07−7.28 (m, 3 H), 7.38−7.60 (m, 2 H). MS (ESI): found $[M + H]^+$, 349.3.

(2*R*,3*S*,4*S*,5*S*,6*R*)-2-(Hydroxymethyl)-6-[4-(4-hydroxyphenyl)-phenoxy]tetrahydropyran-3,4,5-triol (14l). 14l was prepared using the same procedure as for **14e**. Yield: 71%. ^{1}H NMR (300 MHz, methanol-d_4) δ ppm 3.58−3.68 (m, 1 H), 3.69−3.84 (m, 3 H), 3.86−3.97 (m, 1 H), 4.02 (dd, J = 3.43, 1.79 Hz, 1 H), 5.49 (d, J = 1.92 Hz, 1 H), 6.79−6.86 (m, 2 H), 7.11−7.19 (m, 2 H), 7.35−7.42 (m, 2 H), 7.43−7.50 (m, 2 H). MS (ESI): found $[2M + H]^+$, 697.6.

(2*R*,3*S*,4*S*,5*S*,6*R*)-2-(Hydroxymethyl)-6-[4-(2-methoxyphenyl)-phenoxy]tetrahydropyran-3,4,5-triol (14m). 14m was prepared using the same procedure as for **14e**. Yield: 75%. ^{1}H NMR (300 MHz, methanol-d_4) δ ppm 3.60−3.68 (m, 1 H), 3.69−3.83 (m, 6 H), 3.89−3.97 (m, 1 H), 4.03 (dd, J = 3.30, 1.92 Hz, 1 H), 5.52 (d, J = 1.92 Hz, 1 H), 6.94−7.07 (m, 2 H), 7.10−7.17 (m, 2 H), 7.21−7.33 (m, 2 H), 7.37−7.45 (m, 2 H). MS (ESI): found $[M + H]^+$, 363.2.

(2*R*,3*S*,4*S*,5*S*,6*R*)-2-(Hydroxymethyl)-6-[4-(3-methoxyphenyl)-phenoxy]tetrahydropyran-3,4,5-triol (14n). 14n was prepared using the same procedure as for **14e**. Yield: 54%. ^{1}H NMR (300 MHz, methanol-d_4) δ ppm 3.50−3.59 (m, 1 H), 3.60−3.78 (m, 6 H), 3.85 (dd, J = 9.34, 3.30 Hz, 1 H), 3.95 (dd, J = 3.30, 1.92 Hz, 1 H), 5.45 (d, J = 1.65 Hz, 1 H), 6.79 (ddd, J = 8.17, 2.54, 0.82 Hz, 1 H), 6.96−7.16 (m, 4 H), 7.18−7.31 (m, 1 H), 7.38−7.54 (m, 2 H). MS (ESI): found $[M + H]^+$, 363.2.

***N*-[2-[4-[(2*R*,3*S*,4*S*,5*S*,6*R*)-3,4,5-Trihydroxy-6-(hydroxymethyl)-tetrahydropyran-2-yl]oxyphenyl]phenyl]methanesulfonamide (14o). 14o** was prepared using the same procedure as for **14e**. Yield: 63%. ^{1}H NMR (300 MHz, methanol-d_4) δ ppm 2.71 (s, 3 H), 3.57−3.66 (m, 1 H), 3.67−3.83 (m, 3 H), 3.93 (dd, J = 9.34, 3.57 Hz, 1 H), 4.04 (dd, J = 3.43, 1.79 Hz, 1 H), 5.56 (d, J = 1.65 Hz, 1 H), 7.18−7.26 (m, 2 H), 7.26−7.41 (m, 5 H), 7.48 (d, J = 7.69 Hz, 1 H). MS (ESI): found $[M + H]^+$, 426.6.

***N*-[3-[4-[(2*R*,3*S*,4*S*,5*S*,6*R*)-3,4,5-Trihydroxy-6-(hydroxymethyl)-tetrahydropyran-2-yl]oxyphenyl]phenyl]methanesulfonamide (14p). 14p** was prepared using the same procedure as for **14e**. Yield: 52%. ^{1}H NMR (300 MHz, methanol-d_4) δ ppm 2.98 (s, 3 H), 3.56−3.66 (m, 1 H), 3.68−3.83 (m, 3 H), 3.88−3.97 (m, 1 H), 4.03 (dd, J = 3.43, 1.79 Hz, 1 H), 5.53 (d, J = 1.92 Hz, 1 H), 7.17−7.25 (m, 3 H), 7.33−7.42 (m, 2 H), 7.43−7.48 (m, 1 H), 7.50−7.63 (m, 2 H). MS (ESI): found $[M + H]^+$, 426.2.

***N*-Methyl-2-[4-[(2*R*,3*S*,4*S*,5*S*,6*R*)-3,4,5-trihydroxy-6-(hydroxymethyl)tetrahydropyran-2-yl]oxyphenyl]benzenesulfonamide (14q). 14q** was prepared using the same procedure as for **14e**. Yield: 50%. ^{1}H NMR (300 MHz, methanol-d_4) δ ppm 2.36 (s, 3 H), 3.59−3.68 (m, 1 H), 3.68−3.84 (m, 3 H), 3.88−3.96 (m, 1 H), 4.04 (dd, J = 3.43, 1.79 Hz, 1 H), 5.56 (d, J = 1.92 Hz, 1 H), 7.13−7.21 (m, 2 H), 7.28−7.39 (m, 3 H), 7.49−7.58 (m, 1 H), 7.58−7.68 (m, 1 H), 8.03 (dd, J = 7.83, 1.24 Hz, 1 H). MS (ESI): found $[M + H]^+$, 426.1.

***N*-Methyl-3-[4-[(2*R*,3*S*,4*S*,5*S*,6*R*)-3,4,5-trihydroxy-6-(hydroxymethyl)tetrahydropyran-2-yl]oxyphenyl]benzenesulfonamide (14r). 14r** was prepared using the same procedure as for **14e**. Yield: 54%. ^{1}H NMR (300 MHz, methanol-d_4) δ ppm 2.55 (s, 3 H), 3.56−3.66 (m, 1 H), 3.68−3.83 (m, 3 H), 3.89−3.97 (m, 1 H), 4.04 (dd, J = 3.43, 1.79 Hz, 1 H), 5.55 (d, J = 1.92 Hz, 1 H), 7.20−7.30 (m, 2 H), 7.53−7.68 (m, 3 H), 7.77 (dt, J = 8.03, 1.34 Hz, 1 H), 7.82−7.89 (m, 1 H), 8.02 (t, J = 1.79 Hz, 1 H). MS (ESI): found $[M + H]^+$, 426.0.

(2*R*,3*S*,4*S*,5*S*,6*R*)-2-(Hydroxymethyl)-6-[4-(3-nitrophenyl)-phenoxy]tetrahydropyran-3,4,5-triol (14s). 14s was prepared using the same procedure as for **14e**. Yield: 70%. ^{1}H NMR (300 MHz, methanol-d_4) δ ppm 3.61 (ddd, J = 9.75, 4.94, 2.61 Hz, 1 H), 3.68−3.84 (m, 3 H), 3.87−3.98 (m, 1 H), 4.04 (dd, J = 3.43, 1.79 Hz, 1 H), 5.56 (d, J = 1.92 Hz, 1 H), 7.18−7.35 (m, 2 H), 7.57−7.74 (m, 3 H), 7.92−8.08 (m, 1 H), 8.17 (dd, J = 8.24, 2.20 Hz, 1 H), 8.42 (t, J = 2.06 Hz, 1 H). MS (ESI): found $[2M + H]^+$, 755.8.

(2*R*,3*S*,4*S*,5*S*,6*R*)-2-(Hydroxymethyl)-6-[4-(4-nitrophenyl)-phenoxy]tetrahydropyran-3,4,5-triol (14t). 14t was prepared using the same procedure as for **14e**. Yield: 60%. ^{1}H NMR (300 MHz, methanol-d_4) δ ppm 3.56−3.64 (m, 1 H), 3.68−3.84 (m, 3 H), 3.87−3.97 (m, 1 H), 4.04 (dd, J = 3.43, 1.79 Hz, 1 H), 5.57 (d, J = 1.65 Hz, 1 H), 7.20−7.33 (m, 2 H), 7.64−7.76 (m, 2 H), 7.79−7.90 (m, 2 H), 8.24−8.38 (m, 2 H). MS (ESI): found $[M + H]^+$, 378.5.

2-[4-[(2*R*,3*S*,4*S*,5*S*,6*R*)-3,4,5-Trihydroxy-6-(hydroxymethyl)-tetrahydropyran-2-yl]oxyphenyl]benzamide (14u). 14u was prepared using the same procedure as for **14e**. Yield: 42%. It came from the major product of the Suzuki coupling with 2-cyanophenylboronic acid. ^{1}H NMR (300 MHz, methanol-d_4) δ ppm

3.56−3.68 (m, 1 H), 3.68−3.84 (m, 3 H), 3.87−3.97 (m, 1 H), 4.02 (dd, J = 3.30, 1.92 Hz, 1 H), 5.51 (d, J = 1.92 Hz, 1 H), 7.11−7.21 (m, 2 H), 7.33−7.44 (m, 4 H), 7.44−7.57 (m, 2 H). MS (ESI): found $[M + H]^+$, 376.4.

(2*R*,3*S*,4*S*,5*S*,6*R*)-2-(Hydroxymethyl)-6-[4-[2-(trifluoromethyl)-phenyl]phenoxy]tetrahydropyran-3,4,5-triol (14w). 14w was prepared using the same procedure as for **14e**. Yield: 67%. ^{1}H NMR (300 MHz, methanol-d_4) δ ppm 3.60−3.70 (m, 1 H), 3.70−3.86 (m, 3 H), 3.93 (dd, J = 9.34, 3.30 Hz, 1 H), 4.04 (dd, J = 3.30, 1.92 Hz, 1 H), 5.54 (d, J = 1.65 Hz, 1 H), 7.12−7.30 (m, 4 H), 7.34 (d, J = 6.87 Hz, 1 H), 7.47−7.58 (m, 1 H), 7.62 (t, J = 7.14 Hz, 1 H), 7.76 (d, J = 7.97 Hz, 1 H). MS (ESI): found $[2M + H]^+$, 801.8.

(2*R*,3*S*,4*S*,5*S*,6*R*)-2-(Hydroxymethyl)-6-[4-[3-(trifluoromethyl)-phenyl]phenoxy]tetrahydropyran-3,4,5-triol (14x). 14x was prepared using the same procedure as for **14e**. Yield: 70%. ^{1}H NMR (300 MHz, methanol-d_4) δ ppm 3.56−3.66 (m, 1 H), 3.67−3.84 (m, 3 H), 3.93 (dd, J = 9.34, 3.57 Hz, 1 H), 4.03 (dd, J = 3.43, 1.79 Hz, 1 H), 5.55 (d, J = 1.65 Hz, 1 H), 7.17−7.32 (m, 2 H), 7.55−7.66 (m, 4 H), 7.79−7.89 (m, 2 H). MS (ESI): found $[2M + H]^+$, 801.8.

(2*R*,3*S*,4*S*,5*S*,6*R*)-2-[4-(3-Fluorophenyl)phenoxy]-6-(hydroxymethyl)tetrahydropyran-3,4,5-triol (14y). 14y was prepared using the same procedure as for **14e**. Yield: 70%. ^{1}H NMR (300 MHz, methanol-d_4) δ ppm 3.56−3.67 (m, 1 H), 3.68−3.85 (m, 3 H), 3.87−3.97 (m, 1 H), 4.03 (dd, J = 3.43, 1.79 Hz, 1 H), 5.54 (d, J = 1.65 Hz, 1 H), 6.96−7.08 (m, 1 H), 7.14−7.24 (m, 2 H), 7.26−7.35 (m, 1 H), 7.36−7.46 (m, 2 H), 7.51−7.62 (m, 2 H). MS (ESI): found $[2M + H]^+$, 701.8.

***N*1,*N*3-Dimethyl-5-[4-[(2*R*,3*S*,4*S*,5*S*,6*R*)-3,4,5-trihydroxy-6-(hydroxymethyl)tetrahydropyran-2-yl]oxyphenyl]benzene-1,3-dicarboxamide (15b). 15a** (0.050 g, 0.11 mmol) was stirred with 15 mL of $MeNH_2$/EtOH (33 wt %) at room temperature for 40 h. The solvent was removed and the residue was dried in vacuo to afford pure **15b** (0.050 g) in quantitative yield. ^{1}H NMR (300 MHz, methanol-d_4) δ ppm 2.96 (s, 6 H), 3.61−3.66 (m, 1 H), 3.67−3.84 (m, 3 H), 3.86−3.97 (m, 1 H), 4.04 (dd, J = 3.30, 1.92 Hz, 1 H), 5.56 (d, J = 1.92 Hz, 1 H), 7.21−7.34 (m, 2 H), 7.63−7.74 (m, 2 H), 8.13−8.26 (m, 3 H). MS (ESI): found $[M + H]^+$, 447.4.

***N*-Methyl-3-[4-[(2*R*,3*S*,4*S*,5*S*,6*R*)-3,4,5-trihydroxy-6-(hydroxymethyl)tetrahydropyran-2-yl]oxyphenyl]benzamide (14a). 14a** was prepared by direct amination of **8e**, using the same method as for **15b**, in quantitative yield and in pure form. ^{1}H NMR (300 MHz, methanol-d_4) δ ppm 2.94 (s, 3 H), 3.63 (ddd, J = 7.28, 4.81, 2.47 Hz, 1 H), 3.69−3.85 (m, 3 H), 3.87−3.98 (m, 1 H), 4.04 (dd, J = 3.30, 1.65 Hz, 1 H), 5.54 (d, J = 1.92 Hz, 1 H), 7.10−7.27 (m, 2 H), 7.42−7.53 (m, 1 H), 7.54−7.65 (m, 2 H), 7.66−7.79 (m, 2 H), 8.01 (t, J = 1.79 Hz, 1 H). MS (ESI): found $[M + H]^+$, 390.1.

5-[4-[(2*R*,3*S*,4*S*,5*S*,6*R*)-3,4,5-Trihydroxy-6-(hydroxymethyl)-tetrahydropyran-2-yl]oxyphenyl]benzene-1,3-dicarboxylic Acid (15c). 15a (0.025 g, 0.056 mmol) was added into 7 mL of methanol. Then 0.20 M NaOH aqueous (3 mL) was added. The mixture was stirred at room temperature overnight. H^+ exchange resin (DOWEX 50WX4-100) was added to neutralize the mixture. The resin was filtered off and the filtrate was concentrated and then dried in vacuo, giving rise to pure product **15c** (0.023 g) in quantitative yield. ^{1}H NMR (300 MHz, methanol-d_4) δ ppm 3.59−3.67 (m, 1 H), 3.70−3.84 (m, 3 H), 3.94 (dd, J = 3.30, 9.30 Hz, 1 H), 4.05 (dd, J = 3.30, 1.80 Hz, 1 H), 5.56 (d, J = 1.80 Hz, 1 H), 7.26 (m, 2 H), 7.63 (m, 2 H), 8.41 (d, J = 1.50 Hz, 2 H), 8.57 (t, J = 1.50 Hz, 1 H). MS (ESI): found $[M + Na]^+$, 443.0.

3-[4-[(2*R*,3*S*,4*S*,5*S*,6*R*)-3,4,5-Trihydroxy-6-(hydroxymethyl)-tetrahydropyran-2-yl]oxyphenyl]benzoic Acid (14c). 14c was prepared through the hydrolysis of **8e**, using the same method as for **15c**, in quantitative yield and in pure form. ^{1}H NMR (300 MHz, methanol-d_4) δ ppm 3.50−3.60 (m, 1 H), 3.61−3.77 (m, 3 H), 3.81−3.91 (m, 1 H), 3.96 (dd, J = 3.16, 1.79 Hz, 1 H), 5.47 (d, J = 1.65 Hz, 1 H), 7.11−7.20 (m, 2 H), 7.44 (t, J = 7.69 Hz, 1 H), 7.52 (m, J = 8.79 Hz, 2 H), 7.73 (d, J = 7.69 Hz, 1 H), 7.89 (d, J = 7.69 Hz, 1 H), 8.09−8.20 (m, 1 H). MS (ESI): found $[M + H]^+$, 377.5.

3-[(2*R*,3*S*,4*S*,5*S*,6*R*)-3,4,5-Trihydroxy-6-(hydroxymethyl)-tetrahydropyran-2-yl]oxybenzoic Acid (3l). 31 was prepared through the hydrolysis of **3j**, using the same method as for **15c**, in quantitative yield and in pure form. ^{1}H NMR (300 MHz, methanol-d_4) δ ppm 3.52−3.64 (m, 1 H), 3.67−3.83 (m, 3 H), 3.85−3.96 (m, 1 H), 4.03 (dd, J = 3.43, 1.79 Hz, 1 H), 5.55 (d, J = 1.65 Hz, 1 H), 7.32−7.46 (m, 2 H), 7.64−7.78 (m, 2 H). MS (ESI): found $[M + H]^+$, 323.1.

3-[4-[(2*R*,3*S*,4*S*,5*S*,6*R*)-3,4,5-Trihydroxy-6-(hydroxymethyl)-tetrahydropyran-2-yl]oxyphenyl]benzamide (14v). 8e (0.060 g, 0.150 mmol) was stirred in 15 mL of aqueous ammonia (29 wt %) at room temperature for 24 h. The solvent was removed and the residue was purified by HPLC (C18, 15 mm × 150 mm column; eluent acetonitrile/water (0.1% TFA)) to give **14v** (0.037 g) in 65% yield. ^{1}H NMR (300 MHz, methanol-d_4) δ ppm 3.58−3.66 (m, 1 H), 3.69−3.82 (m, 3 H), 3.93 (dd, J = 9.30, 3.30 Hz, 1 H), 4.03 (dd, J = 3.30, 1.50 Hz, 1 H), 5.54 (d, J = 1.80 Hz, 1 H), 7.18−7.26 (m, 2 H), 7.51 (t, J = 7.80 Hz, 1 H), 7.58 − 7.66 (m, 2 H), 7.73−7.83 (m, 2 H), 8.10 (t, J = 1.5 Hz, 1 H). MS (ESI): found $[M + H]^+$, 376.3.

[(2*S*,3*S*,4*S*,5*R*,6*R*)-4,5-Diacetoxy-6-(acetoxymethyl)-2-[4-(9*H*-fluoren-9-ylmethoxycarbonylamino)butoxy]tetrahydropyran-3-yl]-acetate (18). Under nitrogen atmosphere, at 0 °C boron trifluoride diethyl etherate (0.115 g, 0.81 mmol) was added dropwise into a solution of α-D-mannose pentaacetate (0.107 g, 0.27 mmol) and 4-(Fmoc-amino)-1-butanol (0.168 g, 0.54 mmol) in 5 mL of CH_2Cl_2. After a few minutes the mixture was heated to reflux and was kept stirring for more than 36 h. The reaction was then quenched with water and extracted with CH_2Cl_2. The CH_2Cl_2 layer was collected, dried with Na_2SO_4, and concentrated. The resulting residue was purified by silica gel chromography with hexane/ethyl acetate combinations as eluent to give **18** (0.106 g) in 60% yield. ^{1}H NMR (300 MHz, $CDCl_3$) δ ppm 1.48−1.79 (m, 4H), 2.01 (s, 3H), 2.05 (s, 3H), 2.11 (s, 3H), 2.17 (s, 3H), 3.25 (m, 2H), 3.50 (m, 1H), 3.73 (m, 1H), 3.91−4.04 (m, 1H), 4.05−4.18 (m, 1H), 4.18−4.37 (m, 2H), 4.41 (d, J = 6.87 Hz, 2H), 4.74−4.94 (m, 2H), 5.17−5.41 (m, 3H), 7.29−7.37 (m, 2H), 7.37−7.47 (m, 2H), 7.61 (d, J = 7.42 Hz, 2H), 7.78 (d, J = 7.42 Hz, 2H). MS (ESI): found $[M + H]^+$, 642.2.

(2*S*,3*S*,4*S*,5*S*,6*R*)-2-(4-Aminobutoxy)-6-(hydroxymethyl)-tetrahydropyran-3,4,5-triol (19). 18 (0.106 g, 0.165 mmol) was stirred in 6 mL of methanol with a catalytic amount of sodium methoxide (0.02M) at room temperature overnight. The solvent was removed and the residue was purified by silica gel chromatography with a combination of aqueous ammonia and methanol as eluent to afford **19** (0.036 g) in 88% yield. ^{1}H NMR (300 MHz, CD_3OD) δ ppm 1.46−1.78 (m, 4H), 2.61−2.88 (m, 2H), 3.41−3.55 (m, 2H), 3.59 (t, J = 9.3 Hz, 1H), 3.65−3.87 (m, 5H), 4.75 (d, J = 1.65 Hz, 1H). MS (ESI): found $[M + H]^+$, 252.1.

5(6)-FAM-mannoside (20). A mixture of **19** (0.018 g, 0.070 mmol), 5-(and -6)-carboxyfluorescein succinimidyl ester (0.022 g, 0.046 mmol) and triethylamine (0.058 g, 0.57 mmol) in DMF (2 mL) was stirred overnight. After removal of the solvent, the residue was purified by silica gel chromatography with dichloromethane/methanol combination as eluent, giving rise to **20** (0.023 g) in 82% yield. MS (ESI): found $[M + H]^+$, 610.6.

3-[4-[(2*R*,3*S*,4*S*,5*S*,6*R*)-3,4,5-Trihydroxy-6-(hydroxymethyl)-tetrahydropyran-2-yl]oxyphenyl]-*N*-[2-[2-[2-[[3-[4-[(2*R*,3*S*,4*S*,5*S*,6*R*)-3,4,5-trihydroxy-6-(hydroxymethyl)tetrahydropyran-2-yl]-oxyphenyl]benzoyl]amino]ethoxy]ethoxy]ethyl]benzamide (22). Under nitrogen atmosphere, at 0 °C anhydrous DMF (5 mL) was added into the RB flask containing **14c** (0.062 g, 0.165 mmol) and HATU (0.069 g, 0.182 mmol). After the mixture was stirred for 10 min, 1,2-bis(2-aminoethoxy)ethane (0.0123 g, 0.083 mmol) and then *N*,*N*-diisopropylethylamine (0.024 g, 0.182 mmol) were added. The mixture was stirred overnight while being

warmed to room temperature naturally. The solvent was removed and the residue was purified by HPLC (C18, 15 mm × 150 mm column; eluent acetonitrile/water (0.1% TFA)) to give **22** (0.044 g) in 82% yield. ^{1}H NMR (300 MHz, methanol-d_4) δ ppm 3.51−3.65 (m, 6 H), 3.65−3.82 (m, 14 H), 3.88−3.96 (m, 2 H), 4.03 (dd, J = 3.57, 1.92 Hz, 2 H), 5.52 (d, J = 1.65 Hz, 2 H), 7.14−7.24 (m, 4 H), 7.40−7.50 (m, 2 H), 7.53−7.63 (m, 4 H), 7.66−7.77 (m, 4 H), 8.00 (t, J = 1.65 Hz, 2 H). MS (ESI): found $[M + H]^+$, 865.9.

3-[4-[(2*R*,3*S*,4*S*,5*S*,6*R*)-3,4,5-Trihydroxy-6-(hydroxymethyl)-tetrahydropyran-2-yl]oxyphenyl]-*N*-[2-[2-[[3-[4-[(2*R*,3*S*,4*S*,5*S*,6*R*)-3,4,5-trihydroxy-6-(hydroxymethyl)tetrahydropyran-2-yl]oxyphenyl]benzoyl]amino]ethoxy]ethyl]benzamide (21). 21 was prepared using the same method as for **22**. Yield: 76%): ^{1}H NMR (300 MHz, methanol-d_4) δ ppm 3.58−3.66 (m, 6 H), 3.68−3.82 (m, 10 H), 3.93 (dd, J = 9.30, 3.30 Hz, 2 H), 4.03 (dd, J = 3.60, 2.10 Hz, 2 H), 5.53 (d, J = 1.50 Hz, 2 H), 7.14−7.22 (m, 4 H), 7.36−7.42 (m, 2 H), 7.52−7.58 (m, 4 H), 7.64−7.72 (m, 4 H), 7.99 (t, J = 1.50 Hz, 2 H). MS (ESI): found $[M + H]^+$, 821.5.

FimH Fluorescence Polariazation/Anisotropy Assay. Each compound tested was prepared as a 10 mM stock solution in anhydrous DMSO (Sigma, St. Louis, MO) in batches of seven test compounds (plus Butylαman as a positive control) on a 96-well microtiter plate (Evergreen Plastics). Each compound was prepared as a series of 2-fold serial dilutions by the Sciclone robotic liquid handler (Caliper life sciences, Hopkinton, MA) with 11 final compound concentrations ranging from 0 to 10 μM. One microliter of prepared compound was then dry-transferred to each of two 96-well microtiter plates (Corning) which were then filled with 100 μL of assay mixture (200 nM FimH, 20 nM 5(6)-FAM-mannoside (**20**), 50 mM Tris, 100 mM NaCl, 1 mM EDTA, 5 μg BSA, and 5 mM BME). Plates were assayed by reading fluorescence anisotropy using the BioTek Synergy-2 microplate reader (Winooski, VT), taking 100 readings/well using a stabilized tungsten lamp followed by data averaging producing 1 data point per well. Sigma Plot was used for fitting data to a one-site competition binding curve (FP vs compound concentration) to generate an EC_{50} for each compound.

X-ray Crystallography. The adhesin domain of FimH (hereafter "FimH") (residues 1−175 with a C-terminal 6-histidine tag) was cloned into a pTRC99 plasmid and expressed in C600 *E. coli*. FimH was purified from bacterial periplasm by passage over cobalt affinity (Talon, Clontech) and Q Sepharose (GE Healthcare) columns. Protein was subsequently dialyzed against 10 mM MES at pH 6.5, concentrated to 15 mg/mL, and incubated for 30 min with 2 mM compound **8e** prior to cocrystallization. FimH−**8e** crystallized in 20% ethanol, 100 mM imidazole, pH 8.0, and 200 mM $MgCl_2$. Tetragonal bipyramidal crystals measuring 150 μm × 150 μm formed in 2 days and did not diffract unless slowly dehydrated over the course of at least 12 h. Crystals of the FimH−**8e** complex were therefore treated by soaking individual crystals in a stabilizing solution initially containing 15% ethanol, 100 mM imidazole, pH 8.0, 200 mM $MgCl_2$, 10% PEG200, 5% glycerol, and 1 mM compound **8e**. Individual crystals were placed in 150 μL of stabilizing solution in open spot plates and allowed to dehydrate to one-third their original volume over the course of 24 h. Crystals were then harvested without further cryopretection and plunged into liquid nitrogen. Crystals were diffracted to 2.9 Å at beamline 4.2.2 at the Advanced Light Source. Data collection and refinement statistics are summarized in Table 1 of the Supporting Information.

The structure of FimH−**8e** was solved by molecular replacement with the program PHASER[15] using a previously solved model of FimH with its α-D-methylmannoside (Methylαman) ligand removed as the search model (PDB code 1UWF[6a]). There are four FimH−**8e** complexes in the asymmetric unit. Each model of FimH is represented by residues 1−158; further C-terminal residues and the 6-His tag are absent and presumed to be disordered. Each copy of FimH is bound to a single cation, presumed to be calcium from the crystallization condition that is coordinated by Asp-47, the imidazole group of His-45, and water molecules that are not well resolved. All copies of FimH and compound **8e** are essentially the same except for differences in the orientation of the **8e** carboxymethyl group, which in all cases is within hydrogen-bonding distance (2.8−3.0 Å) of the R98/D50 salt bridge. An initial map calculated with $F_o - F_c$ coefficients showed unambiguous difference density for **8e** occupying the extended mannose binding pocket of all four copies of FimH present in the asymmetric unit. Subsequent TLS refinement was performed with REFMAC[16] using chemical restraints for **8e** generated by eLBOW within the PHENIX suite.[17]

Acknowledgment. We appreciate the assistance of Jay Nix at beamline 4.2.2 of the Advanced Light Source with expert data collection. This work was supported in part by the National Institutes of Health (NIH) Grants 1RC1DK086378 and AI048689.

Supporting Information Available: ^{1}H NMR spectra of final compounds and intermediates, FP assay graphical result measuring the K_D of 5(6)-FAM (**20**), and details of the X-ray data collection and refinement of FimH−**8e**. This material is available free of charge via the Internet at http://pubs.acs.org.

References

(1) Waksman, G.; Hultgren, S. J. Structural biology of the chaperone-usher pathway of pilus biogenesis. *Nat. Rev. Microbiol.* **2009**, *7*, 765–774.

(2) (a) Rosen, D. A.; Pinkner, J. S.; Walker, J. N.; Elam, J. S.; Jones, J. M.; Hultgren, S. J. Molecular variations in *Klebsiella pneumoniae* and *Escherichia coli* FimH affect function and pathogenesis in the urinary tract. *Infect. Immun.* **2008**, *76*, 3346–3356. (b) Chen, S. L.; Hung, C. S.; Pinkner, J. S.; Walker, J. N.; Cusumano, C. K.; Li, Z.; Bouckaert, J.; Gordon, J. I.; Hultgren, S. J. Positive selection identifies an in vivo role for FimH during urinary tract infection in addition to mannose binding. *Proc. Natl. Acad. Sci. U.S.A.* **2009**, *106*, 22439–22444. (c) Abraham, S. N.; Sun, D.; Dale, J. B.; Beachey, E. H. Conservation of the D-mannose-adhesion protein among type 1 fimbriated members of the family Enterobacteriaceae. *Nature* **1988**, *336*, 682–684. (d) Martinez, J. J.; Mulvey, M. A.; Schilling, J. D.; Pinkner, J. S.; Hultgren, S. J. Type 1 pilus-mediated bacterial invasion of bladder epithelial cells. *EMBO J.* **2000**, *19*, 2803–2812. (e) Mulvey, M. A.; Lopez-Boado, Y. S.; Wilson, C. L.; Roth, R.; Parks, W. C.; Heuser, J.; Hultgren, S. J. Induction and evasion of host defenses by type 1-piliated uropathogenic Escherichia coli. *Science* **1998**, *282*, 1494–1497. (f) Wright, K. J.; Seed, P. C.; Hultgren, S. J. Development of intracellular bacterial communities of uropathogenic Escherichia coli depends on type 1 pili. *Cell. Microbiol.* **2007**, *9*, 2230–2241. (g) Hung, C. S.; Bouckaert, J.; Hung, D.; Pinkner, J.; Widberg, C.; DeFusco, A.; Auguste, C. G.; Strouse, R.; Langermann, S.; Waksman, G.; Hultgren, S. J. Structural basis of tropism of Escherichia coli to the bladder during urinary tract infection. *Mol. Microbiol.* **2002**, *44*, 903–915.

(3) (a) Mulvey, M. A.; Schilling, J. D.; Hultgren, S. J. Establishment of a persistent *Escherichia coli* reservoir during the acute phase of a bladder infection. *Infect. Immun.* **2001**, *69*, 4572–4579. (b) Anderson, G. G.; Dodson, K. W.; Hooton, T. M.; Hultgren, S. J. Intracellular bacterial communities of uropathogenic Escherichia coli in urinary tract pathogenesis. *Trends Microbiol.* **2004**, *12*, 424–430. (c) Anderson, G. C.; Palermo, J. J.; Schilling, J. D.; Roth, R.; Heuser, J.; Hultgren, S. J. Intracellular bacterial biofilm-like pods in urinary tract infections. *Science* **2003**, *301*, 105. (d) Justice, S. S.; Hung, C.; Theriot, J. A.; Fletcher, D. A.; Anderson, G. G.; Footer, M. J.; Hultgren, S. J. Differentiation and developmental pathways of uropathogenic Escherichia coli in urinary tract pathogenesis. *Proc. Natl. Acad. Sci. U.S.A.* **2004**, *101*, 1333–1338.

(4) Justice, S. S.; Hunstad, D. A.; Seed, P. C.; Hultgren, S. J. Maturation of intracellular escherichia coli communities requires SurA. *Proc. Natl. Acad. Sci. U.S.A.* **2006**, *103*, 19884–19889.

(5) (a) Langermann, S.; Palaszynski, S.; Barnhart, M.; Auguste, G.; Pinkner, J. S.; Burlein, J.; Barren, P.; Koenig, S.; Leath, S.; Jones, C. H.; Hultgren, S. J. Prevention of mucosal escherichia coli infection by FimH-adhesin-based systemic vaccination. *Science* **1997**, *276*, 607–611. (b) Cegelski, L.; Pinkner, J. S.; Hammer, N. D.; Cusumano, C. K.; Hung, C. S.; Chorell, E.; Aberg, V.; Walker, J. N.; Seed, P. C.; Almqvist, F.; Chapman, M. R.; Hultgren, S. J.

Small-molecule inhibitors target Escherichia coli amyloid biogenesis and biofilm formation. *Nat. Chem. Biol.* **2009**, *5*, 913–919.

(6) (a) Bouckaert, J.; Berglund, J.; Schembri, M.; de Genst, E.; Cools, L.; Wuhrer, M.; Hung, C.-S.; Pinkner, J.; Slättegård, R.; Zavialov, A.; Choudhury, D.; Langermann, S.; Hultgren, S. J.; Wyns, L.; Klemm, P.; Oscarson, S.; Knight, S. D.; de Greve, H. Receptor binding studies disclose a novel class of high-affinity inhibitors of the *Escherichia coli* FimH adhesion. *Mol. Microbiol.* **2005**, *55*, 441–455. (b) Gouin, S. G.; Wellens, A.; Bouckaert, J.; Kovensky, J. Synthetic multimeric heptyl mannosides as potent antiadhesives of uropathogenic Escherichia coli. *ChemMedChem* **2009**, *4*, 749–755. (c) Wellens, A.; Garofalo, C.; Nguyen, H.; Van Gerven, N.; Slättegård, R.; Hernalsteens, J.-P.; Wyns, L.; Oscarson, S.; De Greve, H.; Hultgren, S.; Bouckaert, J. Intervening with urinary tract infections using anti-adhesives based on the crystal structure of the FimH-oligomannose-3 complex. *PLoS One* **2008**, *3*, No. e2040. (d) Touaibia, M.; Wellens, A.; Shiao, T. C.; Wang, Q.; Sirois, S.; Bouckaert, J.; Roy, R. Mannosylated G(0) dendrimers with nanomolar affinities to Escherichia coli FimH. *ChemMedChem* **2007**, *2*, 1190–1201. (e) Touaibia, M.; Shiao, T. C.; Papadopoulos, A.; Vaucher, J.; Wang, Q. G.; Benhamioud, K.; Roy, R. Tri- and hexavalent mannoside clusters as potential inhibitors of type 1 fimbriated bacteria using pentaerythritol and triazole linkages. *Chem. Commun.* **2007**, 380–382. (f) Touaibia, M.; Roy, R. Glycodendrimers as anti-adhesion drugs against type 1 fimbriated E. coli uropathogenic infections. *Mini-Rev. Med. Chem.* **2007**, *7*, 1270–1283. (g) Nagahori, N.; Lee, R. T.; Nishimura, S.; Page, D.; Roy, R.; Lee, Y. C. Inhibition of adhesion of type 1 fimbriated Escherichia coli to highly mannosylated ligands. *ChemBioChem* **2002**, *3*, 836–844. (h) Furneaux, R. H.; Pakulski, Z.; Tyler, P. C. New mannotriosides and trimannosides as potential ligands for mannose-specific binding proteins. *Can. J. Chem.* **2002**, *80*, 964–972. (i) Lindhorst, T. K.; Kieburg, C.; Krallmann-Wenzel, U. Inhibition of the type 1 fimbriae-mediated adhesion of Escherichia coli to erythrocytes by multiantennary alpha-mannosyl clusters: the effect of multivalency. *Glycoconjugate J.* **1998**, *15*, 605–613. (j) Kotter, S.; Krallmann-Wenzel, U.; Ehlers, S.; Lindhorst, T. K. Multivalent ligands for the mannose-specific lectin on type 1 fimbriae of Escherichia coli: syntheses and testing of trivalent alpha-D-mannoside clusters. *J. Chem. Soc., Perkin Trans. 1* **1998**, 2193–2200. (k) Sperling, O.; Fuchs, A.; Lindhorst, T. K. Evaluation of the carbohydrate recognition domain of the bacterial adhesin FimH: design, synthesis and binding properties of mannoside ligands. *Org. Biomol. Chem.* **2006**, *4*, 3913–3922.

(7) Firon, N.; Ashkenazi, S; Mirelman, D.; Ofek, I.; Sharon, N. Aromatic alpha-glycosides of mannose are powerful inhibitors of the adherence of type 1 fimbriated *Escherichia coli* to yeast and intestinal epithelial cells. *Infect. Immun.* **1987**, *55*, 472–476.

(8) Meuwly, R.; Vasella, A. Synthesis of 1,2-cis-configurated glycosylphosphonates. *Helv. Chim. Acta* **1986**, *69*, 25–34.

(9) (a) Hultgren, S. J.; Duncan, J. L.; Schaeffer, A. J.; Amundsen, S. K. Mannose-sensitive haemagglutination in the absence of piliation in *Escherichia coli*. *Mol. Microbiol.* **1990**, *4*, 1311–1318. (b) Slonim, L. N.; Pinkner, J. S.; Branden, C. I.; Hultgren, S. J. Interactive surface in the PapD chaperone cleft is conserved in pilus chaperone superfamily and essential in subunit recognition and assembly. *EMBO J.* **1992**, *11* (13), 4747–56.

(10) Baker, N. A.; Sept, D.; Joseph, S; Holst, M. J.; McCammon, J. A. Electrostatics of nanosystems: application to microtubules and the ribosome. *Proc. Natl. Acad. Sci. U.S.A.* **2001**, *98*, 10037–10041.

(11) Topliss, J. G. Utilization of operational schemes for analog synthesis in drug design. *J. Med. Chem.* **1972**, *15* (10), 1006–1011.

(12) (a) Cusumano, C. K.; Hultgren, S. J. Bacterial adhesion. A source of alternate antibiotic targets. *IDrugs* **2009**, *12*, 699–705. (b) Cegelski, L.; Marshall, G. R.; Eldridge, G. R.; Hultgren, S. J. The biology and future prospects of antivirulence therapies. *Nat. Rev. Microbiol.* **2008**, *6* (1), 17–27.

(13) Ernst, B.; Magnani, J. L. From carbohydrate leads to glycomimetic drugs. *Nat. Rev. Drug Discovery* **2009**, *8*, 661–677.

(14) Kogan, T. P.; Dupre, B.; Bui, H.; McAbee, K. L.; Kassir, J. M.; Scott, I. L.; Hu, X.; Vanderslice, P.; Beck, P. J.; Dixon, R. A. F. Novel synthetic inhibitors of selectin-mediated cell adhesion: synthesis of 1,6-bis[3-(3-carboxymethylphenyl)-4-(2-α-D-mannopyranosyloxy)phenyl]hexane (TBC1269). *J. Med. Chem.* **1998**, *41*, 1099–1111.

(15) McCoy, A. J.; Grosse-Kunstleve, R. W.; Adams, P. D.; Winn, M. D.; Storoni, L. C.; Read, R. J. Phaser crystallographic software. *J. Appl. Crystallogr.* **2007**, *40*, 658–674.

(16) Murshudov, G. N.; Vagin, A. A.; Dodson, E. J. Refinement of macromolecular structures by the maximum-likelihood method. *Acta Crystallogr., Sect. D: Biol. Crystallogr.* **1997**, *53*, 240–55.

(17) Moriarty, N. W.; Grosse-Kunstleve, R. W.; Adams, P. D. Electronic ligand builder and optimization workbench (eLBOW): a tool for ligand coordinate and restraint generation. *Acta Crystallogr., Sect. D: Biol. Crystallogr.* **2009**, *65*, 1074–1080.